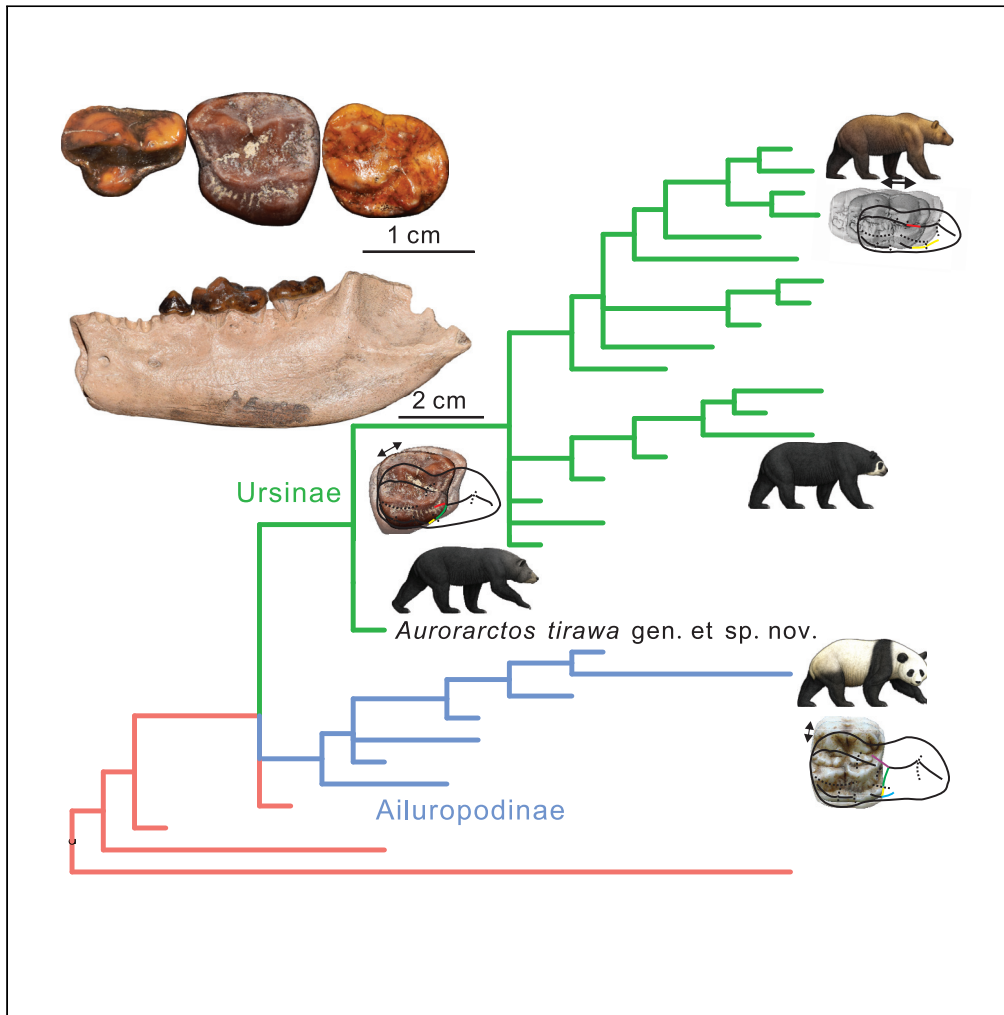


Article

The Earliest Ursine Bear Demonstrates the Origin of Plant-Dominated Omnivory in Carnivora



Qigao Jiangzuo,
John J. Flynn

jiangzuo@ivpp.ac.cn

HIGHLIGHTS

We describe the earliest known ursine bear, supported by phylogenetic analyses

The new fossil bear has the earliest evidence of plant-dominated omnivory diet

We discuss how traits helped ursine bears breaking energetic limitations on body size



Article

The Earliest Ursine Bear Demonstrates the Origin of Plant-Dominated Omnivory in Carnivora

Qigao Jiangzuo^{1,2,3,4,5,*} and John J. Flynn⁴

SUMMARY

In Carnivora, increases in body size often lead to dietary specialization toward hypercarnivory. Ursine bears (*Tremarctos* and *Ursus*), however, are the only omnivorous Carnivora that evolved large body sizes (i.e., >50 kg). Traits contributing to their gigantism, and how those traits evolved, have never been studied. Here we propose that special dental characters of Ursinae (parallel buccal and lingual ridges) permit a sagittally oriented mastication associated with increasing emphasis on plant foods. This pattern can be traced back to a new early diverging bear of plant-dominated omnivorous diet, *Aurorarctos tirawa* gen. et sp. nov. from the late Middle Miocene of North America, which was supported as the earliest known ursine bear by phylogenetic analysis. The anatomical transition to increased masticatory efficiency, probably together with the ability to hibernate, helped bears break prior ecological limitations on body size and led to the evolution of a distinctive lineage of herbivorous-omnivorous, large-bodied Carnivora.

INTRODUCTION

Adaptation to omnivory, which increases the flexibility of diet choice from a dominantly carnivorous ancestry, repeatedly evolved within Carnivora (Ewer, 1973). Most omnivorous Carnivora lineages, e.g. Melinae and Taxidiinae in Mustelidae (Ginsburg and Morales, 2000); most members of Procyonidae (Baskin, 1998a); *Conepatus* and *Mydaus* in Mephitidae (Baskin, 1998b); *Nyctereutes* and the extinct clades Phlaocyoni and Cynarctina in Canidae (Wang et al., 1999; Tedford et al., 2009); and Paradoxurinae in Viverridae (Ewer, 1973), however, retain small or medium sizes, seldom reaching a body mass larger than 20 kg, suggesting the presence of ecological or morphological constraints on body mass in omnivorous Carnivora. Analyses of fossil Canidae suggested that selection for larger body sizes would lead to dietary specialization for hypercarnivory (Van Valkenburgh et al., 2004). Similarly, all large terrestrial fossil musteloids, i.e. *Megalictis* (Valenciano et al., 2016), large Guloninae (Harrison, 1981; Valenciano et al., 2018), Mellivorinae (Valenciano et al., 2015), the large ailurid *Simocyon* (Wang, 1997), and the large procyonid *Chapalmalania* (Forasiepi et al., 2014), are hypercarnivores (and often with bone-crushing adaptation). This phenomenon is correlated with energetic constraints on body mass or maximal rate of energy expenditure, since terrestrial Carnivora (except bear) that are larger than 21.5 kg (or slightly larger if the animal has lower basal metabolism rate) can only live upon on large vertebrate prey than smaller invertebrate prey (Carbone et al., 1999; McNab, 2000). This body mass threshold on species relay on small prey can be extended to omnivorous diet species that include significant plant items, because carnivores, including even the most herbivorous member (the giant panda *Ailuropoda melanoleuca*), do not have a digestive tract, digestive enzymes, or a gut microbiota well adapted to eating plant material (Nie et al., 2019).

The high energetic requirement and low efficiency in digesting plant food may limit omnivorous Carnivora in evolving large body sizes. Bears (Ursidae) are the exception to the general covariance of large size and Carnivora within Carnivora, with omnivorous ursine lineages evolving to very large sizes, often greater than 100 kg. Energetic demands in large-bodied taxa can be reduced by the ability to hibernate during the cold season (Hellgren, 1998). This behavior, however, cannot explain why only bears evolved a large body size, because hibernation also is present in several omnivorous musteloids, e.g. badgers and skunks (Geiser, 2013). We propose that bears initially evolved a unique masticatory pattern to increase digestive efficiency associated with an omnivorous diet with increasing plant components, which in conjunction with evolution

¹Key Laboratory of Vertebrate Evolution and Human Origins of Chinese Academy of Sciences, Institute of Vertebrate Paleontology and Paleoanthropology, Chinese Academy of Sciences, Beijing 100044, China

²CAS Center for Excellence in Life and Paleoenvironment, Beijing 100044, China

³University of Chinese Academy of Sciences, Beijing 100049, China

⁴Division of Paleontology, American Museum of Natural History, New York 10024, USA

⁵Lead Contact

*Correspondence: jiangzuo@ivpp.ac.cn

<https://doi.org/10.1016/j.isci.2020.101235>



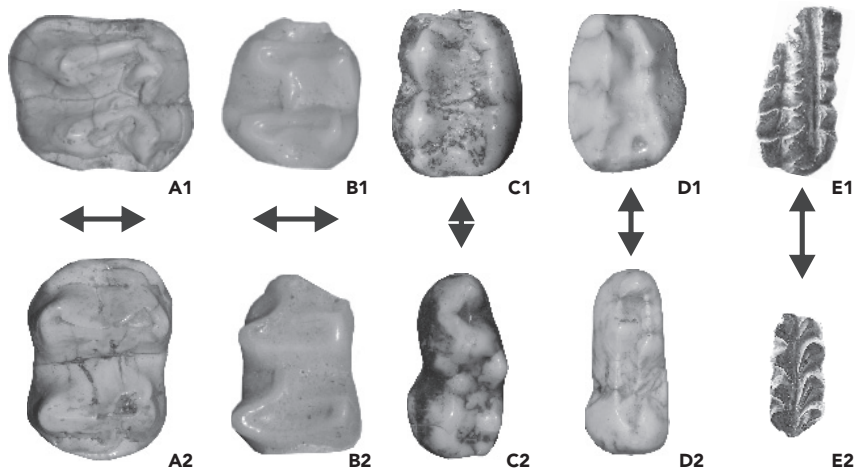


Figure 1. Masticatory Pattern of Various Mammals, as Reflected by M1/m1 Morphology

(A1 and A2) giant tapir *Megatapirus augustus* (Perissodactyla) AMNH FM1-8754; (B1 and B2) brush-tail rock-wallaby *Petrogale penicillata* (Marsupialia) AMNH CA2869; (C1 and C2) spectacled bear *Tremarctos ornatus* (Carnivora) AMNH M67732; (D1 and D2) Asiatic black bear *Ursus thibetanus* (Carnivora) IVPP V5601.22 (reversed) and IVPP V5711.4. (E1 and E2) *Lambdopsalis bulla* (Multituberculata) IVPP V20101. Not to scale. Arrows indicate masticatory direction. Note the sagittally oriented ridges of grooves in *Ursus thibetanus* and to a lesser extent in *Tremarctos ornatus* (lower m1 with incomplete lingual ridge).

of the ability to hibernate ultimately permitted the evolution of large body sizes even in these omnivorous-herbivorous taxa. There are two derived dental characters in Ursini that clearly increase masticatory efficiency. One is anteroposterior elongation of the posterior molars, specifically M2 and m2, and another is a shift of the masticatory pattern from the ancestral, more transverse chewing direction (latero-medial) to a derived, more sagittal direction (antero-posterior). The latter character is rather distinctive among Mammalia, because most species with increasing grinding functions develop transverse ridges (Figures 1A and 1B). How these two characters evolved is uncertain, however, because early fossil ursine bears have been unknown and no phylogeny has been performed regarding the origins of ursine species and clades.

Here we report a substantial sample of an early diverging North American bear, from late Middle Miocene-aged (~15–12.5 million-year-old) fossil sites in Nebraska (see Supplemental Information for geological background details) housed in UNSM (University of Nebraska State Museum, Lincoln, Nebraska, U.S.A.), which was preliminarily identified as *Ursavus cf. brevirohinus* by Hunt (1998). Some traits of this bear are unique to Ursinae, and our analyses suggest that this bear is a new taxon distinct from *Ursavus* and represents the earliest known member of the Ursinae. It also provides new information for reconstructing initial character states relating to evolution of the unique masticatory pattern of later ursine bears.

Materials and methods, abbreviations, etc. are presented at the end of this manuscript. Two living subfamilies, Ailuropodinae and Ursinae, with the latter being further subdivided into the tribes Ursini and Arctotheriini, are recognized (here we follow (Qiu et al., 2014)).

RESULTS

Systematics

Ursidae Fischer [de Waldheim], 1814 Ursinae Fischer [de Waldheim], 1814

Aurorarctos gen. nov.

Etymology: named after “Aurora,” dawn in Latin, and “Arctos,” for bear in Greek.

Type species: *Aurorarctos tirawa* sp. nov.

Referred species: so far only known from the type species.

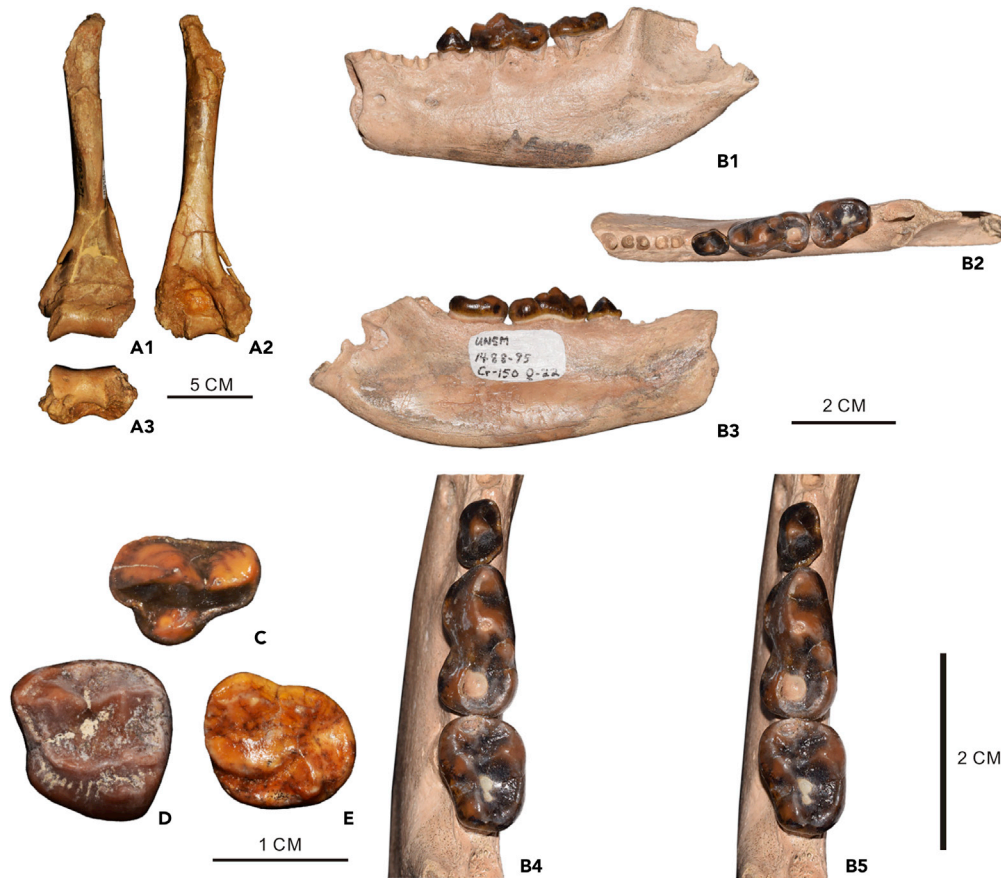


Figure 2. Specimens of *Aurorarctos tirawa* gen. et sp. nov.

(A1–A3) UNSM45118, partial humerus, anterior (A1), posterior (A2), and distal (A3) views; (B1–B5) UNSM95237 holotype mandible; B1, buccal view; B2, occlusal view; B3, lingual view; B4–5, stereophotograph of occlusal surfaces of the dentition; (C) UNSM95211, P4, occlusal view; (D) UNSM95209, M1, occlusal view; (E) UNSM95206, M2, occlusal view.

Aurorarctos tirawa sp. nov. (Figure 2)

Ursavus cf. *brevirhinus* (Hunt, 1998)

Etymology: species named after Tirawa, the god of creation for the Pawnee people of the Great Plains.

Holotype: UNSM95237, a left mandible with p4–m2 preserved. (UNSM = University of Nebraska State Museum).

Referred material: see [Supplemental Information](#).

Type locality: Stewart Quarry (Cr150) in Cherry County, northern Nebraska, USA.

Chronology: so far only known from the Late Barstovian (~15–12.5 Ma) North American Land Mammal “Age” (NALMA).

Diagnosis: small-sized species of early diverging Ursinae. Mandible robust and deepens posteriorly. Premolar series complete; p2–p4 double-rooted; mandible lacking premasseteric fossa or marginal process; P4 lacking parastyle and protocone, and inner lobe located on anterior half of tooth; M1 wide with strong postero-lingual, cusp-like cingulum; M2 with short talon, weak antero-medial accessory ridge of paracone and connected protocone and metacone; p4 with lingual ridge and non-subdivided posterior ridge; m1 with postero-lingual ridge of protocone anteriorly curved, with initial posterior ridge, and variable

presence of postero-buccal ridge of protocone, and entoconid often weakly or not subdivided; m2 with wide trigonid and separated paraconid.

Differential Diagnosis

Differs from the genotype species for *Ursavus*, *U. brevirohinus*, in having a more massive P4 paracone; wider M1 with strong postero-lingual corner; m1 with anteriorly curved RPrd3 (postero-medial ridge of the protoconid, detailed meaning see (Jiangzuo et al., 2019) and presence of RPrd2 (posterior ridge of the protoconid), with a stronger buccal concavity between the trigonid and talonid; m2 with much wider trigonid and separated paraconid; differs from *U. primaevus* in smaller size; proportionally shorter M2 talon and connected protocone-metacone; m1 with an anteriorly curved RPrd3 and presence of RPrd2; differs from *Ursavus pawniensis* in smaller size and less elongated m2 with stronger buccal concavity; differs from *Ballusia* spp. in larger size with longer M2 talon and derived m1 characters (especially protoconid region); differs from Late Miocene *Ursavus* species, e.g. *Ursavus tedfordi*, in smaller size, much larger premolars, larger and more anteriorly located inner lobe of P4, shorter M2 talon, and non-subdivided p4 posterior ridge.

For detailed description and comparison of the fossil material pertaining to this new species, see [Supplemental Information](#).

Phylogenetic Analysis

Phylogenetic analyses of fossil and living bears have been conducted separately on Ailuropodinae (Abella et al., 2012) and Ursinae (Wang et al., 2017), but neither of those studies focused on stem group taxa or was inclusive across Ursidae and thus are not suitable as a comprehensive framework for understanding the relationships and significance of the new taxon. We therefore developed a new character-taxon phylogenetic matrix emphasizing inclusion of more taxa from the stem group of Ursinae. Our new matrix contains 130 craniodental characters and one humerus character (which is the only postcranial character that can be applied to the new species described here). A total of 31 taxa were included, including all living species of Ursidae, with the extant wolf *Canis lupus* as the outgroup. For details of the character matrix, see the [Supplemental Information](#).

In the phylogenetic analyses, Maximum Parsimony and Bayes Inference (with and without topological constraint, see [Methods](#) for details) methods yield similar topologies and support *Aurorarctos tirawa* as a stem ursine ([Figures S6–S8](#)). For relationships within the Ursini, we applied a topological constraint for the relationship of living species of *Ursus* such as *Ursus thibetanus*, *Ursus malayanus*, *Ursus ursinus*, *Ursus americanus*, *Ursus arctos*, and *Ursus maritimus*, because this topology has been independently confirmed by both a genome-wide phylogeny (Kumar et al., 2017) and a phylogeny based on transposable element insertions (Lammers et al., 2017). Our final tree, used for further analyses, is based on the Bayes Inference phylogeny because this method allows a different evolution rate for each traits, which makes sense ([Figure 3](#)).

Ursavus is definitely polyphyletic in our phylogenetic analysis, and none of the other previously recognized species of *Ursavus* link in an exclusive clade with the genotype species, which is a basal ursid far removed from all the other species previously assigned to *Ursavus*. Thus, we recognize a new genus and species for the basalmost ursine taxon (previously preliminarily recognized as “*Ursavus* cf. *brevirohinus*” by Hunt, 1998 and herein named *Aurorarctos tirawa*), and all other “*Ursavus*” species besides the genotype have the genus name in quotation marks, reflecting likely nonmonophyly of this genus. Species previously assigned to this genus include the stem ursid *Ursavus brevirohinus* (the genotype species), stem ailuropodine “*Ursavus*” *primaevus*, stem ursine *Aurorarctos tirawa*, and three other ursine species (“*U.*” *ehrenbergi*, “*U.*” *sylvestris*, and “*U.*” *tedfordi*) that form a polytomy with the Arctotheriini and Ursini clades. “*Ursavus*” *tedfordi* may represent a stem species of Ursini; although this is not resolved by our phylogenetic analysis, because of character conflict suggesting potential affinities with either Ursini or Arctotheriini, the presence of a distinct marginal process and subdivided p4 posterior ridge may support its potential Ursini affinity (Jiangzuo et al., 2019). In addition to its basal position within the Ursinae, *Aurorarctos tirawa* is morphologically very primitive and thus well exemplifies the ancestral craniodental conditions for ursine evolution.

DISCUSSION

Paleoecology of *Aurorarctos tirawa*

The paleoecology of the new fossil ursine species can be inferred from four lines of evidence: depth of the mandibular ramus, dental features, caries pits, and morphology of the humerus distal articular surface.

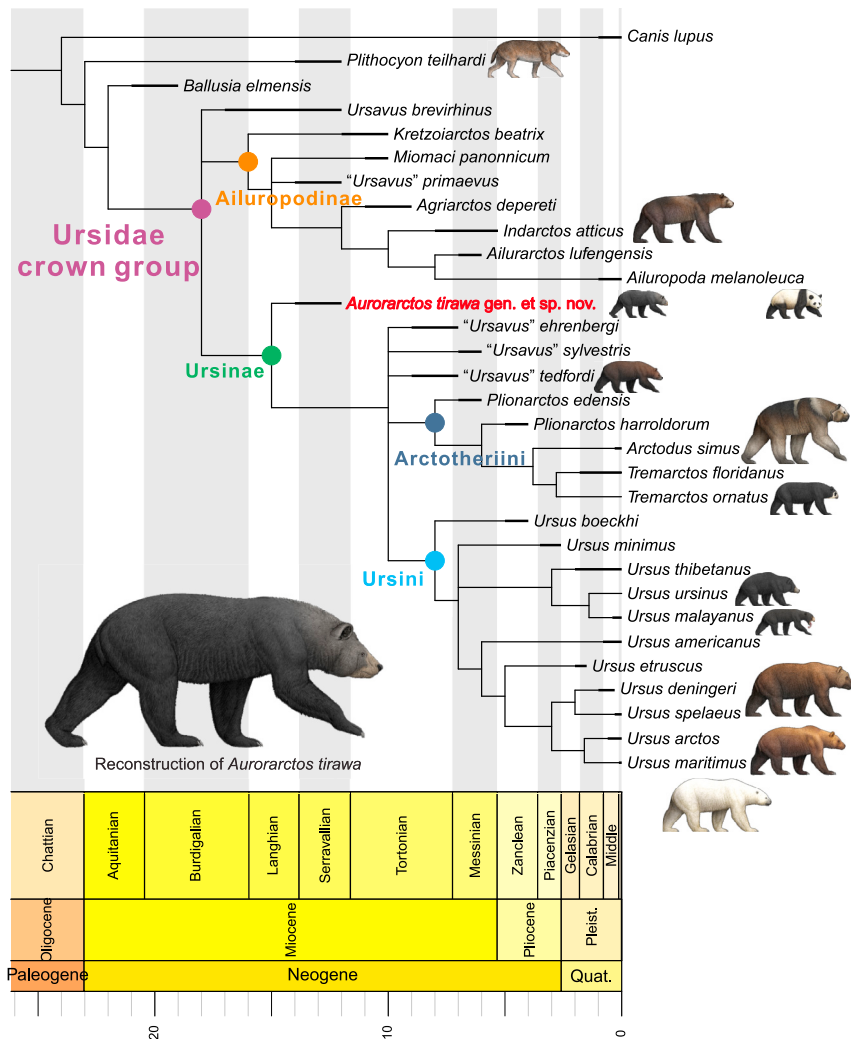


Figure 3. Bayesian Inference Phylogenetic Tree of Ursidae, with a Life Reconstruction of *Aurorarctos tirawa* gen. et sp. nov.

Note that we apply the total group (crown group + stem group) usage of Ailuropodinae, Ursinae, Ursini, and Arctotheriini. Artwork by Yu Chen.

Compared with the complex suite of masticatory and neurosensory functions of the cranium, the mandible functioned only in feeding and thus can be especially useful for inferring paleodiet (Herring, 1993; Piras et al., 2013). In general, a deeper mandibular ramus is correlated with increasing loading resistance (Therrien, 2005). *Aurorarctos tirawa* has a rather deep mandible (the ratio of m1 versus mandible depth behind m1 is 0.64), close to the relative depth in living bears (see Table S2), in contrast to a much more slender mandible in the earlier stem ursid *Ballusia elmensis* (ratio = 0.92 according to (Dehm, 1950). Geometric morphometric analysis (Figure 4) also suggests that *Ballusia* falls within the morphospace occupied by the carnivorous/insectivorous-omnivorous group, whereas *Aurorarctos tirawa* is located within the range of herbivorous/herbivorous-omnivorous extant bears. This suggests that the origin of an herbivorous-omnivorous diet in living bears evolved through a transitional stage, exemplified by *Ballusia*, of an insectivorous-omnivorous diet, and that the herbivorous-omnivorous specialization of ursines already had been acquired by the appearance of the earliest representative of Ursinae, *Aurorarctos tirawa*.

Dental characters also support an omnivorous diet for *Aurorarctos tirawa*. The cusps of *Aurorarctos tirawa* teeth are blunt and low-crowned. It is especially noteworthy that the pair of m1 entoconids commonly seen in Miocene Ursidae tend to be fused in *A. tirawa*. This character decreases the puncturing ability relative to

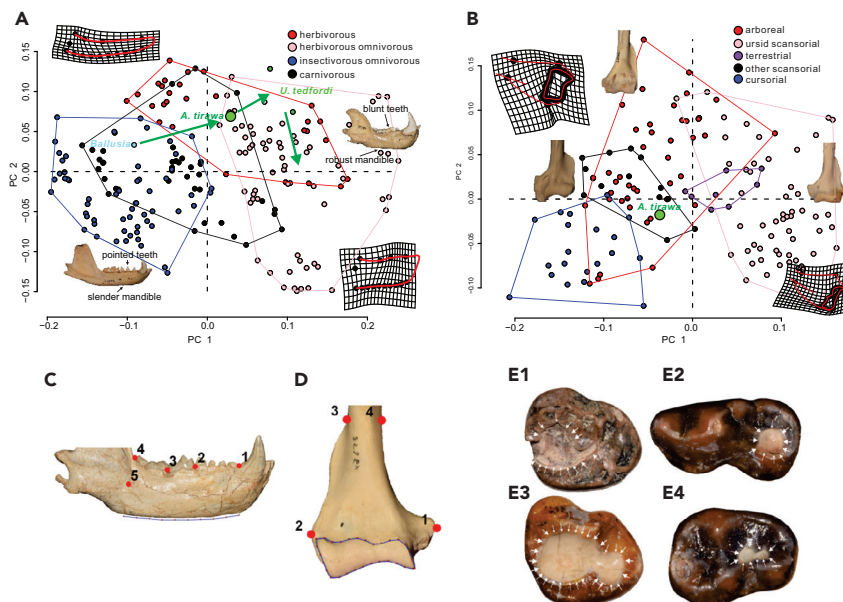


Figure 4. Geometric Morphometric Analyses (PCA) of *Aurorarctos tirawa* and Related Carnivora, and Evidence of Dental Caries in the New Taxon

(A) Geometric morphometric analysis of mandible profile; (B) geometric morphometric analysis of distal humerus; (C) mandible landmarks (in this figure, the semilandmarks were shifted slightly lower than the mandible ventral contour for improved visibility); (D) distal humerus landmarks; (E) dental caries (boundary marked by white arrows) in four molars of *Aurorarctos tirawa*: E1 UNSM95200, E2 UNSM95237, E3 UNSM45086, E4 UNSM95237.

that seen in insectivorous carnivores, such as mongooses (Herpestidae), badgers (*Meles/Arctonyx*), and the fossil stem ursid *Ballusia*. An omnivorous diet is further supported by the presence of dental caries. Large pits are frequently present in the trigon/trigonid or talon/talonid basins, as observed in three (representing four teeth, see Figure 4A) of the total of 14 specimens of this new taxon that preserve teeth. Evidence of dental caries is distinct from the normal wear pattern of the teeth, which begins at the apices of the cusps rather than from within the basin. In all four of these teeth, the apices have much weaker wear than the basin, so basin pitting clearly represents dental caries. Dental caries is common in living bears (Hall, 1945; Jin et al., 2015) and has been observed in several fossil ursine bears (Gross, 1931; Soibelzon et al., 2014; Wang et al., 2017). The extremely high frequency of dental caries (21.4% in *Aurorarctos tirawa*, much higher than in extant bears (2% according to Hall (1945)), indicates that this fossil bear probably relied heavily on sugar-rich fruits in its diet.

All extant ursine bears have a relatively robust metapodial system and employ a plantigrade gait. In contrast, most of the common Early and Middle Miocene bears, usually classified as Hemicyoninae, are digitigrade with elongated limbs (Frick, 1926; Ginsburg and Morales, 1998). Little is known of the postcrania of *Ballusia* or species of *Ursavus*, because their fossils are almost exclusively represented by isolated teeth or jaw fragments. One exception is the late Early Miocene species *Ballusia orientalis* from the Shanwang Biota in Shandong Province, eastern China (Qiu et al., 1985). That species has whole skeletons preserved and exhibits slender postcranial bones that differ markedly from living bears but are somewhat similar in proportions to hemicyonids (Qiu et al., 1985). Therefore, there are large morphological gaps between the early stem ursid *Ballusia* and living ursine and ailuropodine bears. When the body plan typical of extant ursine bears evolved has been unknown. The humerus of *Aurorarctos tirawa*, although incomplete, provides useful information on the locomotor pattern of this earliest-diverging ursine. Its deltoid tuberosity is greatly extended along most of the humerus, with overlap of its distal part with the lateral epicondyle of the humerus in the shaft, just as in living bears (Davis, 1964), and the epicondyle also is well developed, although not so expanded as in extant ursine bears. The trochlea facet also is similar to living bears, with a weak trochlea ridge. The antero-posterior depth of the humeral condyle is shallower than in extant bears (Figure 2). There are two other major differences between *Aurorarctos tirawa* and extant bears. The first is the presence of a large entepicondyle foramen. This foramen is absent in Ursini and present but smaller in

Arctotheriini (Erdbrink, 1953; Davis, 1964; Hunt, 1998). The second is the overall more slender form of the humerus in *A. tirawa*, in both the epicondyle and shaft. To investigate the potential locomotor style of *A. tirawa*, we performed a geometric morphometric analysis of the distal humerus (Figures 4B and 4D). The results clearly suggest that *A. tirawa* is distinct from living scansorial bears as well as cursorial Carnivora, but falls into the morphospace of small, arboreal-fossorial Carnivora such as *Arctictis*, *Ailurus*, *Nasua*, *Meles*, and *Taxidea*, but its epicondyle is definitely weaker than that of fossorial badger. Overall, the anatomy of the humerus (see details in Supplemental Information) suggests that *Aurorarctos tirawa* most likely was an arboreal member of the Carnivora.

In summary, *Aurorarctos tirawa* had a unique ecological habitat relative to the stem ursid *Ballusia* and to extant bears, in its distinctive combination of herbivorous-omnivorous and arboreal adaptations. In contrast, *Ballusia*, the nearest relative of crown Ursidae probably was more insectivorous-omnivorous and terrestrial. This suggests that the scansorial habitus of living ursines is not directly evolved from a terrestrial ancestor as was estimated by the ancestral state reconstruction for living species (see Figure S16), through a badger-like body plan, but instead stemmed from an arboreally adapted body plan. This fossil-based inference is further supported by the observation that most medium-sized extant bears still retain substantial abilities to climb trees (Fitzgerald and Krausman, 2002).

Origin of the Unique Bear Masticatory Pattern

We propose that in bears the two derived ursine dental characters mentioned in the introduction are correlated, because the shift to a more sagittally oriented masticatory pattern can generate higher masticatory antero-posterior efficiency, which in turn favors selection toward antero-posteriorly elongated molars. This shift of masticatory pattern in ursines can now be reconstructed as having been achieved by sequential opening of the protoconid-metaconid connection of the m1 (Figure 5A), which represents the original anterior boundary of m1 movement during mastication (Figure 5-B1), permitting occlusal motion in an antero-posterior direction unimpeded by a transverse crest. In *Aurorarctos tirawa*, the postero-medial ridge (RPrd3) is anteriorly curved, opening additional space for antero-posterior movement (Figure 5-B2). Arctotheriini generally retain their m1 morphology at this state (or slightly more derived), but most living Ursini species are more derived in the ultimate loss of RPrd3, permitting full development of the antero-posterior masticatory pattern without any transverse barrier for such movement (Figure 5-B3). The only living *Ursus* species retaining a connected protoconid-metaconid is the sun bear *Ursus malayanus* (Figure 5A), which also retains less elongated posterior molars relative to other species of *Ursus*, indicating that this crest was lost independently several times in the *Ursus* lineage or that a similar connection evolved again only in *U. malayanus* after ancestral loss in Ursini. We map the length ratios of M2/M1 and m2/m1 on the phylogenetic tree to trace the elongation of molars in Ursidae (Figures 5C and 5D). In the basal ursine *Aurorarctos tirawa*, M2/m2 are not elongated, but in other Ursinae, especially Ursini, M2/m2 are distinctly elongated. In contrast, Ailuropodinae only have a weakly or moderately elongated M2/m2, as in *Aurorarctos tirawa*. Species with a more derived RPrd3 (state 0 is not anteriorly curved, 1 is anteriorly curved, and 2 is loss of RPrd3) also generally have a longer M2/m2 (Figure 5E). Phylogenetic generalized least squares analyses of the ratios of M2/M1 and m2/m1 relative to the m1 RPrd3 character state also support a positive significant correlation between the two former traits. This suggests that the transition from the original posteriorly curved state through the intermediate anteriorly curved state to final loss of the m1 RPrd3 is a key innovation that permitted a shift of masticatory direction more antero-posteriorly, and in turn favored antero-posterior elongation of the posterior molars, permitting more efficient mastication in an increasingly herbivorous-omnivorous lineage and evolution of larger body sizes. In contrast, Ailuropodinae retain the primitive condition for the RPrd3 and a strong postglenoid process (Figure S17) that restricts antero-posterior jaw movements, and this clade of large bears employed a different pathway to increase masticatory efficiency, i.e., transversely widening the molars without changing the jaw biomechanics. This innovation seems to be less efficient than that of Ursinae, as the largest terminal herbivorous taxon *Ailuropoda melanoleuca*, which is specialized in skull, dental, postcranial, and physiology (Davis, 1964; Endo et al., 1999; Nie et al., 2015), is still not comparable Ursinae in body size (Figure S18). The unique pattern of increased masticatory efficiency in Ursinae documented by the new stem ursine taxon and ancestral state character reconstructions, followed by or together with evolution of the ability to hibernate, helped ursine bears break the energetic and ecological constraint on body size for herbivorous-omnivorous Carnivora and contributed to their later success as distinctive large-bodied herbivores-omnivores in the dominantly carnivorous Carnivora clade.

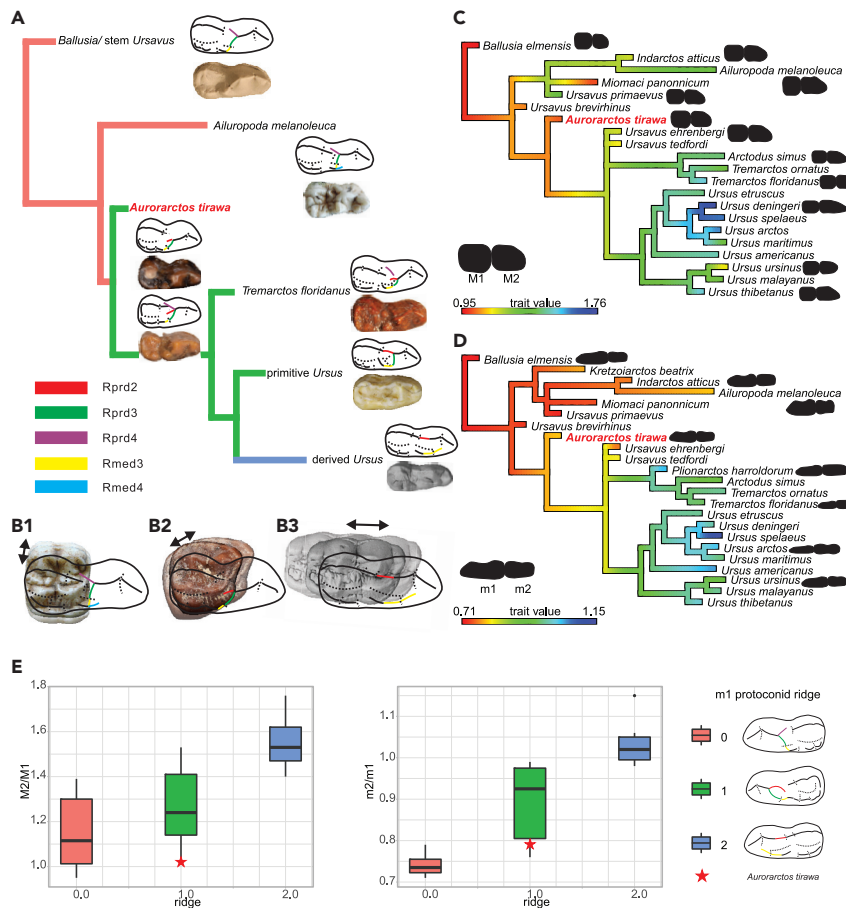


Figure 5. Dental Evolution in Ursidae

(A) Evolution of the m1 protoconid region.

(B1–B3) P4/m1 occlusion relationships in three taxa, representing the shift of jaw biomechanics-masticatory direction in bears; B1, *Ailuropoda* spp. (representing the ancestral condition for ursids); B2, *Aurorarctos tirawa*; B3, *Ursus deningeri*.

(C) Evolution of ratio of M2 length versus M1 length along the phylogenetic tree (Figure 2).

(D) Evolution of ratio of m2 length versus m1 length along the phylogenetic tree (Figure 2); (E) boxplots of the ratios of M2/M1 length and m2/m1 length, relative to different states of m1 postero-lingual ridge (state 0 is not anteriorly curved, 1 is anteriorly curved, and 2 is loss of RPrd3).

Limitations of the Study

In this study, we performed the phylogenetic analysis mainly based on dental traits, as the new fossil only has these remains. A more detailed functional analysis would be ideal pending on the discovery of more fossil material. Our codings of European species *Ursavus brevirhinus* and *Ursavus primaevus* are only based on materials from type localities, and materials from other localities are probably heterogenous and need a more systematic review. Our explanation about body size evolution and dietary change still lacks a very robust statistical support, as most fossil species only have very limited material, and physiological factors (e.g. hibernation, basal metabolism rate) cannot be tested for fossil species.

Resource Availability

Lead Contact

Qigao Jiangzuo, jiangzuo@ivpp.ac.cn.

Materials Availability

The fossils are housed in the University of Nebraska State Museum, Lincoln, Nebraska, U.S.A.

Data and Code Availability

The data are available in the [Supplemental Information](#).

METHODS

All methods can be found in the accompanying [Transparent Methods supplemental file](#).

SUPPLEMENTAL INFORMATION

Supplemental Information can be found online at <https://doi.org/10.1016/j.isci.2020.101235>.

ACKNOWLEDGMENTS

We thank R. Hunt Jr, R. Secord, and G. Corner for allowing studying the specimen and for their help during the senior author's visit in UNSM; J. Meng, R. O'Leary, and J. Galkin for their help in accessing the AMNH fossil mammal collections; M. Surovy, E. Hoeger, and S. Ketelsen for their help in accessing the AMNH modern mammal collections; Z. Qiu and J. Chen for help in accessing fossil collections of the IVPP; X. Zhu and Y. Yang for help in accessing IOZ modern mammal collection; X. Jiang for help in accessing KIZ modern mammal collection. We thank Y. Chen for reconstruction of fossil and living bear appearances. We thank F. Mao and H. Wang for discussing the masticatory pattern of Multituberculata and providing photos of *Lambdopsalis bulla*. We thank editor and reviews suggestions, which greatly improve the quality of this work. This work was supported by the Strategic Priority Research Program of Chinese Academy of Sciences (Grant No. XDB26000000 and XDA20070203), Key Frontier Science Research Program of the Chinese Academy of Sciences (Grant Nos. QYZDY-SSW-DQC-22 and GJHZ1885), the National Natural Science Foundation of China (Grant Nos. 41430102, 41872001, 41872005 and 41772018), Paleontological Society student grant (USA), and China Scholarship Council in award to the senior author (QJ) and by the Frick Fund of the Division of Paleontology at AMNH.

AUTHOR CONTRIBUTIONS

Q. Jiangzuo performs the phylogenetic analysis and systematic work. Q. Jiangzuo and J. Flynn perform the paleoecological analysis. Q. Jiangzuo and J. Flynn wrote the manuscript.

DECLARATION OF INTERESTS

The authors declare no competing interests.

Received: February 1, 2020

Revised: April 26, 2020

Accepted: May 29, 2020

Published: June 26, 2020

REFERENCES

- Abella, J., Alba, D.M., Robles, J.M., Valenciano, A., Rotgers, C., Carmona, R., Montoya, P., and Morales, J. (2012). *Kretzoiarctos* gen. nov., the oldest member of the giant panda clade. *PLoS One* 7, 1–7.
- Baskin, J.A. (1998a). 8 Procyonidae. In *Evolution of Tertiary Mammals of North America: Terrestrial Carnivores, Ungulates, and Ungulate-like Mammals*, C.M. Janis, K.M. Scott, and L.L. Jacobs, eds. (Cambridge University Press), pp. 144–151.
- Baskin, J.A. (1998b). 9 Mustelidae. In *Evolution of Tertiary Mammals of North America: Terrestrial Carnivores, Ungulates, and Ungulate-like Mammals*, C.M. Janis, K.M. Scott, and L.L. Jacobs, eds. (Cambridge University Press), pp. 152–173.
- Carbone, C., Mace, G.M., Roberts, S.C., and Macdonald, D.W. (1999). Energetic constraints on the diet of terrestrial carnivores. *Nature* 402, 286–288.
- Davis, D.D. (1964). *The Giant Panda: A Morphological Study of Evolutionary Mechanisms* (Chicago Natural History Museum, Fieldiana: Zoology memoirs), p. 3.
- Dehm, R. (1950). Die Raubtiere aus dem Mittel-Miocän (Burdigalium) von Wintershof-West bei Eichstätt in Bayern (Bayerische Akademie der Wissenschaften), p. 58.
- Endo, H., Yamagiwa, D., Hayashi, Y., Koie, H., Yamaya, Y., and Kimura, J. (1999). Role of the giant panda's 'pseudo-thumb'. *Nature* 397, 309–310.
- Erdbrink, D. (1953). A Review of Fossil and Recent Bears of the World with Remarks on Their Phylogeny Based on Their Dentition (Drukkerij Jan de Lange).
- Ewer, R.F. (1973). *The Carnivores* (Cornell University Press).
- Fitzgerald, C.S., and Krausman, P.R. (2002). *Helarctos malayanus*. *Mamm. Species* 696, 1–5.
- Forasiépi, A.M., Soibelzon, L.H., Gomez, C.S., Sánchez, R., Quiroz, L.I., Jaramillo, C., and Sánchez-Villagra, M.R. (2014). Carnivorans at the Great American Biotic Interchange: new discoveries from the northern neotropics. *Naturwissenschaften* 101, 965–974.
- Frick, C. (1926). The Hemicyoninae and an American tertiary bear. *Bull. Am. Mus. Nat. Hist.* 56, 1883–1965.
- Geiser, F. (2013). Hibernation. *Curr. Biol.* 23, R188–R193.
- Ginsburg, L., and Morales, J. (1998). Les Hemicyoninae (Ursidae, Carnivora, Mammalia) et

- les formes apparentées du Miocène inférieur et moyen d'Europe occidentale. *Ann. Paléontol.* 84, 71–123.
- Ginsburg, L., and Morales, J. (2000). Origine et évolution des Melineae (Mustelidae, Carnivora, Mammalia). *Comptes Rendus de l'Académie des Sciences Paris, Sciences de la Terre et des planètes/Earth and Planetary Sciences*, vol. 330, pp. 221–225.
- Gross, J. (1931). Kiefer-und Zahnerkrankungen bei *Ursus spelaeus* R. (Nach den Funden aus der Potocnikhöhle in der Uschowa). *Centralblatt f. Min. etc., Abt. B* 4, 187–190.
- Hall, E.R. (1945). Dental caries in wild bears. *Trans. Kans. Acad. Sci.* (1903-) 48, 79–85.
- Harrison, J.A. (1981). A Review of the Extinct Wolverine, *Plesiogulo* (Carnivora, Mustelidae) from North America (Smithsonian Institution Press).
- Hellgren, E.C. (1998). Physiology of hibernation in bears. *Ursus* 10, 467–477.
- Herring, S.W. (1993). Functional morphology of mammalian mastication. *Am. Zool.* 33, 289–299.
- Hunt, R.M., Jr. (1998). 10 Ursidae. In *Evolution of Tertiary Mammals of North America: Terrestrial Carnivores, Ungulates, and Ungulatelike Mammals*, C.M. Janis, K.M. Scott, and L.L. Jacobs, eds. (Cambridge University Press), pp. 174–195.
- Jiangzuo, Q., Liu, J., and Chen, J. (2019). Morphological homology, evolution and proposed nomenclature for bear dentition. *Acta Palaeontol. Pol.* 64, 693–710.
- Jin, Y., Chen, S., Chao, Y., Pu, T., Xu, H., Liu, X., Zhao, K., Nie, Y., Wei, W., and Lin, D. (2015). Dental abnormalities of eight wild Qinling giant pandas (*Ailuropoda melanoleuca qinlingensis*), Shaanxi Province, China. *J. Wildl. Dis.* 51, 849–859.
- Kumar, V., Lammers, F., Bidon, T., Pfenninger, M., Kolter, L., Nilsson, M.A., and Janke, A. (2017). The evolutionary history of bears is characterized by gene flow across species. *Sci. Rep.* 7, 46487.
- Lammers, F., Gallus, S., Janke, A., and Nilsson, M.A. (2017). Phylogenetic conflict in bears identified by automated discovery of transposable element insertions in low-coverage genomes. *Genome Biol. Evol.* 9, 2862–2878.
- McNab, B.K. (2000). Energy constraints on carnivore diet. *Nature* 407, 584.
- Nie, Y., Wei, F., Zhou, W., Hu, Y., Senior, A.M., Wu, Q., Yan, L., and Raubenheimer, D. (2019). Giant pandas are macronutritional carnivores. *Curr. Biol.* 29, 1677–1682.e2.
- Nie, Y.G., Speakman, J.R., Wu, Q., et al. (2015). Exceptionally low daily energy expenditure in the bamboo-eating giant panda. *Science* 349, 171–174.
- Piras, P., Maiorino, L., Teresi, L., Meloro, C., Lucci, F., Kotsakis, T., and Raia, P. (2013). Bite of the cats: relationships between functional integration and mechanical performance as revealed by mandible geometry. *Syst. Biol.* 62, 878–900.
- Qiu, Z.X., Deng, T., and Wang, B.Y. (2014). A late Miocene *Ursavus* skull from Guanghe, Gansu, China. *Vert. Palae.* 52, 265–302.
- Qiu, Z.X., Yan, D.F., Jia, H., and Wang, B.Z. (1985). Dentition of the *Ursavus* skeleton from Shanwang, Shandong province. *Vert. Palae.* 23, 264–271.
- Soibelzon, L.H., Grinspan, G.A., Bocherens, H., Acosta, W.G., Jones, W., Blanco, E.R., and Prevosti, F. (2014). South American giant short-faced bear (*Arctotherium angustidens*) diet: evidence from pathology, morphology, stable isotopes, and biomechanics. *J. Paleontol.* 88, 1240–1250.
- Tedford, R.H., Wang, X., and Taylor, B.E. (2009). Phylogenetic systematics of the north american fossil caninae (Carnivora: Canidae). *Bull. Am. Mus. Nat. Hist.* 325, 1–218.
- Therrien, F. (2005). Mandibular force profiles of extant carnivorans and implications for the feeding behaviour of extinct predators. *J. Zool.* 267, 249–270.
- Valenciano, A., Abella, J., Alba, D.M., Robles, J.M., Álvarez-Sierra, M.A., and Morales, J. (2018). New early Miocene material of *Iberictis*, the oldest member of the wolverine lineage (Carnivora, Mustelidae, Guloninae). *J. Mamm. Evol.* 27, 73–93.
- Valenciano, A., Abella, J., Sanisidro, O., Hartstone-Rose, A., Álvarez-Sierra, M.A., and Morales, J. (2015). Complete description of the skull and mandible of the giant mustelid *Eomellivora piveteaui* Ozansoy, 1965 (Mammalia, Carnivora, Mustelidae), from Batallones (MN10), late Miocene (Madrid, Spain). *J. Vertebr. Paleontol.* 35, e934570.
- Valenciano, A., Baskin, J.A., Abella, J., Pérez-Ramos, A., Álvarez-Sierra, M.A., Morales, J., and Hartstone-Rose, A. (2016). *Megalictis*, the bone-crushing giant mustelid (Carnivora, Mustelidae, Oligobuninae) from the early Miocene of North America. *PLoS One* 11, 1–26.
- Van Valkenburgh, B., Wang, X., and Damuth, J. (2004). Cope's rule, hypercarnivory, and extinction in North American canids. *Science* 306, 101–104.
- Wang, X. (1997). New cranial material of Simocyon from China, and its implications for phylogenetic relationship to the red panda (*Ailurus*). *J. Vertebr. Paleontol.* 17, 184–198.
- Wang, X., Tedford, R.H., and Taylor, B.E. (1999). Phylogenetic systematics of the Borophaginae (Carnivora: Canidae). *Bull. Am. Mus. Nat. Hist.* 243, 1–391.
- Wang, X.M., Rybczynski, N., Harington, C.R., White, S.C., and Tedford, R.H. (2017). A basal ursine bear (*Protarctos abstrusus*) from the Pliocene High Arctic reveals Eurasian affinities and a diet rich in fermentable sugars. *Sci. Rep.* 7, 1–14.

iScience, Volume 23

Supplemental Information

**The Earliest Ursine Bear Demonstrates
the Origin of Plant-Dominated
Omnivory in Carnivora**

Qigao Jiangzuo and John J. Flynn

Transparent Methods

Institutional abbreviations

AMNH American Museum of Natural History, New York, U.S.A.

AMNH CA specimens of living species from Vertebrate Paleontology collection of American Museum of Natural History, New York, U.S.A.

AMNH F:AM Frick fossil mammal collection of American Museum of Natural History, New York, U.S.A.

AMNH FM fossil mammal collection of American Museum of Natural History, New York, U.S.A.

AMNH M Mammal collection of American Museum of Natural History, New York, U.S.A.

HMV Hezheng fossil Museum, Gansu, China.

IOZ Institute of Zoology, Chinese Academy of Sciences, Beijing, China

IVPP Institute of Vertebrate Paleontology and Paleoanthropology, Chinese Academy of Sciences, Beijing, China, with specimen capitalized with V (fossil specimens) or OV (living specimens)

KIZ Kunming Institute of Zoology, Chinese Academy of Sciences, Kunming, Yunnan, China

MN European Neogene land mammal age

NHMW Naturhistorisches Museum Wien, Vienna, Austria

NMP National Museum, Prague, Czech Republic

SFNR Shaanxi Foping National Reserve, Foping, Shanxi, China

SW Shandong Linqu Shanwang Paleontological Museum, Linqu, Shandong,
China

UNSM University of Nebraska State Museum, Lincoln, Nebraska, U.S.A.

USNM Department of Paleobiology, Smithsonian Institution, Washington, D.C.,
U.S.A.

UW Department of Palaeontology, [Universität Wien](https://www.univie.ac.at), Vienna, Austria

Materials

Specimens of the new species described in this study come from three localities in Nebraska, all from the Late Barstovian NALMA, i.e., late Middle Miocene age (~15-12.5 Ma). The material is represented by two mandibles, 14 isolated teeth, and one partial humerus housed in the University of Nebraska State Museum.

For comparison, we checked specimens of all eight living species of bears (Ursidae); five living species of mustelids (*Meles meles*, *Meles leucurus*, *Arctonyx collaris*, *Arctonyx albogularis* and *Gulo gulo*); three living species of canid (*Nyctereutes procyonoides*, *Canis adustus* and *Lycalopex vetulus*) housed in the collections of the AMNH, IOZ, IVPP, KIZ and SFNR. We also studied fossil bears, including *Plithocyon teilhardi*, *Plithocyon ursinus* and *Phoberocyon johnhenryi* housed in AMNH FM collections, *Ballusia orientalis* housed in SW; *Ursavus primaevus* and *Ursavus ehrenbergi* (cast) housed in AMNH FM; *Ursavus pawniensis* housed in AMNH; *Ursavus tedfordi* housed in HNV; *Ursavus sylvestris* housed in IVPP;

Indarctos spp. housed in NHMW, IVPP, HVM and AMNH FM; *Agriarctos depereti* (cast) housed in UW; *Ailurarctos lufengensis* housed in IVPP; *Plionarctos edensis*, *Tremarctos floridanus* and *Arctodus simus* from AMNH FM and USNM; *Ursus boeckhi* (cast) in UW; *Ursus etruscus* in IVPP and AMNH FM; *Ursus deningeri* and *Ursus spelaeus* fossils in NMP and UW also were checked for comparison. Specimen numbers and other details are provided in the Appendix.

Methods

The terms of dental structure follow Jiangzuo et al. (2019) (see Appendix Fig. S2) and dental measurement standards are shown in Appendix Fig. S18.

For the phylogenetic analysis, we performed a maximum parsimony analysis (Traditional search, TBR 1000 replicates) in the software package TNT 1.5 (Goloboff et al., 2008; Goloboff and Catalano, 2016) (<http://www.lillo.org.ar/phylogeny/tnt/>) and Bayes Inference (Mkv model, 10 million generations, burnin 0.25) in Mrbayes 3.2.6 (Huelsenbeck and Ronquist, 2001; Ronquist et al., 2012). Both analyses were run with and without molecular backbone constraints ((*Ursus thibetanus* (*Ursus malayanus*, *Ursus ursinus*))(*Ursus americanus*, (*Ursus arctos*, *Ursus maritimus*))).

Parts of figure plots were made in the software package ggplot2(Wickham, 2016) in R(R Development Core Team, 2016). The phylogenetic tree was rescaled by chronological age using the package paleotree(Bapst, 2012). Characters were mapped into the tree using the package phytools(Revell, 2012). Phylogenetic generalized linear model was performed using the package nlme(Pinheiro et al., 2013). Geometric morphometric analyses were performed using the package geomorph(Adams and Otá

rola - Castillo, 2013). Ancestor state reconstruction was performed in package ape (Muda and Othman, 2015). All packages noted in this paragraph were implemented in R.

Geological background

The material described in this study comes from three localities in Nebraska, all from the Late Barstovian age, i.e. the late Middle Miocene (~15-12.5 Ma). Of the three localities, two are located in northern Nebraska, West Valentine Quarry (Cr114) and Stewart Quarry (Cr150); another one, Myers Farm (Wt15A) is from southern Nebraska (Fig. S1).

Terminology

Dental terminology follows Jiangzuo et al. (2019). For a graphic summary, see Fig. S2.

Systematics

Description

The holotype mandible UNSM95237 from Cr-150 Q22 preserves most of the horizontal ramus with the p4–m2. The ramus is moderately robust and high, and deepens slightly posteriorly. Two subequal-sized mental foramina are present in the preserved part, nearly at the same height. The anterior one is located below the p2 and the posterior one at the level between the p3 and p4. There is no premasseteric fossa, but in the corresponding place, the mandible is slightly concave. The masseteric fossa extends to the level of the m3. The symphysis seems to only extend to the level of the p1. The medial face of the mandible is slightly concave posteriorly. The mandibular foramen is located relatively high, only slightly lower than the tooth row. The marginal process is absent, and the scar for the pterygoid muscle is weakly indicated at this place.

All premolars are present without any diastema, but these premolars are not imbricated, as indicated by the alveoli. The p1 is single-rooted whereas the p2–p4 are double-rooted. The p4 is stout, surrounded by a weak cingulid. No accessory cuspids are present. The p4 buccal contour is slightly concave, and the lingual contour is convex. A distinct ridge is present in the lingual wall of the main cuspid of p4. The m1 is robust. The m1 cingulid is only weakly developed, occurring at the buccal side of the trigonid

and the antero-buccal side of the talonid. There is a prominent buccal constriction between the trigonid and talonid of m1. The postero-buccal ridge of the m1 protoconid is weakly developed and connected to the anterior end of the hypoconid; the postero-lingual ridge connecting with the metaconid is slightly anteriorly curved. A tiny additional posterior ridge of the m1 protoconid is also present, starting from the apex and quickly disappearing. The m1 hypoconid and entoconid are similar in height, and the entoconid is not subdivided. There is a large caries pit in the m1 talonid basin. The m2 has a massive trigonid with an enlarged trigonid basin. The m2 metaconid is slightly higher than the protoconid. The m2 paraconid and premetaconid are weakly differentiated. The m2 talonid is distinctly narrower than the trigonid, and the entoconid is not subdivided as in the m1. There are two small caries pits in the m2, one on the anterior border of the trigonid basin and another on the buccal side of the talonid basin. The m3 is single-rooted.

Another edentulous mandible, UNSM95205 from Cr114, is very similar to that of the holotype but is slightly larger. The position of the two mental foramina is exactly the same as that of the holotype.

Beyond the two above-mentioned mandibles, there are several isolated teeth, described next.

P4: Two isolated P4s are known. UNSM95211 is an unworn P4 from Cr114. The cingulum is well developed and surrounds the tooth except the inner lobe and posterior side of the metacone. The anterior border of the paraconid is obtuse. The antero-lingual ridge is present and connects to the boundary between the paracone and the inner lobe. The inner lobe is moderately in size and located at the anterior part of the tooth. The hypoconid is the sole cusp in the inner lobe, with its apex inner the posterior ridge of the paracone. UNSM95210 is slightly worn. The morphology is not different from that of UNSM95211.

M1: Three isolated M1s are known. UNSM95207 is the only unworn one, and serves as the primary basis for this description. This tooth is rather wide. The width across the paraconid is distinctly smaller than across the metacone. The buccal cingulum is well developed, whereas the lingual cingulum is only developed at the postero-lingual side of the tooth where it is cusp-like. The parastyle and metastyle are absent. The paracone is slightly shorter than the metacone. The medial ridge of the paracone is weak, whereas the medial ridge of the metacone is well developed and extends to the central valley. The protocone and metaconule form a continuous ridge, with the separation between the two located at the level of the anterior ridge of the metacone. The postprotocrista-metaconule is nearly parallel to the paracone-metacone ridge. There is a small transverse ridge between the paracone and protocone. The medial and lateral slopes of the protocone-metaconule ridge are similar in width. Both slopes bear many rugose small ridges perpendicular to the protocone-metaconule ridge. The second M1, UNSM95208, is moderately worn and very similar in structure to UNSM95207. The lingual cingulum is more anteriorly extended compared with that of UNSM95207, however, and there is a small transverse ridge between the paracone and protocone. UNSM95209 is a lightly worn M1. This tooth probably experienced some post-mortem abrasion and, as a result, nearly all enamel is missing so no character

details can be seen.

M2: Four isolated M2s are known. Both UNSM 95206 and UNSM95212 are well preserved and unworn. The UNSM95212 M2 is distinctly more antero-posteriorly elongated than any of the known M1s. It bears a distinct but short talonid. Its width across the paracone is distinctly wider than across the metacone. There is a distinct buccal concavity between the paracone and metacone, and the paracone is distinctly longer than the metacone. There is a weak transverse ridge starting from the anterior ridge of the paracone. The posterior ridge of the metacone turns buccally. The protocone forms a lingually curved ridge, with its anterior part parallel to the paracone, whereas the posterior part turns buccally and connects with the medial ridge of the metacone. The metaconule is fused with the lingual cingulum; its anterior ridge connects with the postprotocrista. The lingual cingulum is moderately developed, extending along the entire lingual part of the tooth. UNSM 95206 is similar to UNSM95212, but the buccal concavity between the paracone and metacone is weaker, and the antero-medial ridge of the metaconule turns more buccally in the former. UNSM95200 is a slightly worn M2, that is very close in morphology to UNSM95206. A small wrinkle in the lingual slope of the protocone is distinct. There is a large caries pit occupying the entire trigon basin. UNSM45086 from is a moderately worn M2. The contour of the tooth is very similar to that of UNSM95212. Both the trigon and talon basins are marked by large caries pits.

m1: Two additional isolated m1s and an m1 fragment are known. UNSM95213 is unworn, but the buccal part of the talonid is slightly broken. A buccal cingulid is present on the antero-buccal side of the trigonid. The posterior part of the trigonid shows a combination of noteworthy characters. A distinct mesoconid ridge is present at the buccal base of the protoconid, and its anterior end connects with the postero-buccal ridge of the protoconid. The antero-lingual ridge of the protoconid is anteriorly curved as in UNSM95237. The posterior ridge is small but distinct, and is more extended than in UNSM95237, approaching the valley between the protoconid and metaconid. The hypoconid bears a distinct posterior ridge turning lingually to reach the entoconid, closing the talonid basin posteriorly. The entoconid is subdivided into two cuspids, with the anterior one being slightly larger. UNSM95224 is larger than the other m1s. The lingual concavities between the paraconid and metaconid and between metaconid and entoconid are stronger than on other m1s. Cingulids are present on the antero-buccal side of the trigonid and the buccal side of the talonid. The mesoconid ridge and postero-buccal ridge of the protoconid are present but indistinct. The postero-lingual ridge of the protoconid is anteriorly curved, as in other m1s. The posterior ridge that occurs in the other two isolated m1s is absent in UNSM95224. The talonid is robust. The entoconid is not subdivided. UNSM95214 is an m1 talonid fragment, and its entoconid also is not subdivided.

m2: Only one isolated m2, UNSM95215, is known. This tooth has a rather wide trigonid and a narrower talonid. The buccal constriction is strong, whereas the lingual constriction is weak. The paraconid is distinct from the protoconid, and the metaconid is higher than the protoconid. The posterior ridge of the protoconid is not subdivided. The entoconid is ridge-like and not subdivided.

Humerus: A partial humerus, UNSM45118 (Fig. 1-a1–a3), represents the only known postcranial bone for this new taxon. The distal 2/3 of the humerus is preserved, but the distal condyle is broken. The humerus is moderately robust and relatively small (widest part of distal humerus = 57.67 mm). The deltoid tuberosity is well developed, extends rather far distally, and its distal border overlaps with the proximally extended ectepicondyle in the shaft. The distal condyle is expanded, with a well-developed epicondyle. There is a large and elongated entepicondylar foramen. The trochlea facet is moderately thick. The proximal border forms three proximally-convex curves and two distally concave notches. The distal border of the trochlea is smoothly concave, with a moderately developed trochlea ridge. The olecranon fossa is laterally inclined and shallow in posterior view, and the entire condyle is shallow in distal view.

Comparisons

The material of *Aurorarctos tirawa* described above represents a small-sized, Miocene-aged bear comparable in size to the stem ursid *Ursavus brevirohinus*. The mandible height is smaller than that of any living bear, as well as that of “*U.*” *tedfordi*, but is comparable to a large-sized extant wolverine. The body mass of this new fossil bear is thus estimated to be ~10–20 kg.

Ursavus brevirohinus is the genotype species of *Ursavus*. This species was first discovered from Voitsberg in Austria (MN5) and erected as *Cephalogale brevirohinus* by Hofmann (1887). It was referred to *Hyaenarctos* by Hofmann (1892) when he described new material from Steiermark, Austria. Schlosser (1899) selected this species as the type species of his new genus *Ursavus*. More material of this species were later found from Kieferstadel (Wegner, 1913), Göriach (Thenius, 1949) and Can Llobateres (Crusafont Pairó and Kurtén, 1976), though the latter record is much younger and probably represents another species. *Aurorarctos tirawa* is close in size to *U. brevirohinus*, and is similar in having unreduced premolars and M2 with a short talon, but is distinct in having a more massive P4 paracone, wider M1 with a strong posterolingual corner, m1 with an anteriorly curved RPrd3 and presence of RPrd2 and a stronger buccal concavity between the trigonid and talonid, and an m2 with a much wider trigonid and separation of the paraconid.

Another European Middle Miocene species, “*Ursavus*” *primaevus* is known from slightly younger deposits, best represented by specimens from La Grive Saint Alban (Gaillard, 1899; Schlosser, 1899). This species is distinguished from *A. tirawa* in its larger size, proportionally longer M2 talon, m1 lacking an anteriorly curved RPrd3, and absence of RPrd2.

The Early Miocene *Ballusia* (Dehm, 1950; Qiu et al., 1985; Ginsburg and Morales, 1998), “*Ursavus*” *hareni*, and “*Ursavus*” *isorei*⁸ are generally more anatomically primitive than *A. tirawa* in their smaller size, shorter M2 talon, and lacking the derived m1 characters of *A. tirawa* described above.

The Late Miocene “*Ursavus*” species mostly fall far from the genotype species (a basal ursid), instead lying nested well within the crown group of Ursidae, being either early members of Ursinae or Ailuropodinae (Fig. 2). Thus, those other species should

no longer be placed in *Ursavus*, as that would render the genus polyphyletic. The best known Late Miocene “*Ursavus*” species is the late Bahean-aged “*Ursavus*” *tedfordi* from Huaigou, Hezheng area, northern China (Qiu et al., 2014). This species is represented by a beautifully preserved, complete skull (including an associated mandible). This species, was postulated by Qiu et al. (2014) and Jiangzuo et al. (2019) to be an early member of Ursini, as it has a small marginal process in the mandible and the posterior ridge of the p4 is subdivided, but in our analysis lies in an unresolved polytomy with two other “*Ursavus*” species, Arctotheriini, and Ursini. “*U.*” *tedfordi* is larger than *A. tirawa*, and much more anatomically derived in having more reduced premolars, smaller and more posteriorly situated inner lobe of the P4, more rounded M1, longer M2 talon, and subdivided p4 posterior ridge. A slightly younger species, “*Ursavus*” *sylvestris* from Lufeng, southwestern China (Qi, 1984; Qiu and Qi, 1990), has a similar morphology to that of “*U.*” *tedfordi*, though the P4 inner lobe is smaller, thus differing even more substantially from *A. tirawa*. Another Ursini species is “*Ursavus*” *ehrenbergi* from Europe, known mainly by a maxilla from Halmyropotamos, Greece (Thenius, 1947), of MN11 age. A mandible from Perivolaki referred to “*Ursavus*” *depereti* (Koufos, 2006) shows typical ursine characters and according to our analysis likely belongs to “*U.*” *ehrenbergi*. In general, “*U.*” *ehrenbergi* has a similar evolutionary grade to that of “*U.*” *tedfordi* and “*U.*” *sylvestris*, falling together in an unresolved polytomy near the base of Ursinae, but the M2 is further enlarged and is different significantly from *A. tirawa*, the most basal taxon within Ursinae (Fig. 2).

Two additional genera previously considered to be *Ursavus*-like bears are known from the Late Miocene, i.e. *Agriarctos* from Europe (Kretzoi, 1942; Viret, 1949; Thenius, 1979) and *Ailurarctos* from East Asia (Qiu and Qi, 1989; Zong, 1997). Both genera here are viewed as Ailuropodini (Qiu et al., 2014) (Fig. 2), and are distinct from and much more derived than *A. tirawa* in having well developed accessory cusps/cuspids in the premolars, an especially large ridge-like P4 parastyle, and a much more complicated occlusal surface in the molars. Only one genus is known from the Late Miocene in North America, *Plionarctos* (Tedford and Martin, 2001). The species *P. edensis* is the earliest known Arctotheriini (Fig. 2), and it is more anatomically derived than *A. tirawa* in its larger size, more posteriorly located P4 inner lobe, larger m2 and M2 with longer talon, and presence of a mesoconid on m1.

In summary, *A. tirawa* differs from all known species of *Ursavus* or *Ursavus*-like Miocene bear. It is more anatomically derived than any Early Miocene species in a number of features, but less derived than any Late Miocene species in several other characters. Most Late Miocene species can be assigned to one of the two tribes of extant ursine bears (Arctotheriini, Ursini) or to the Ailuropodinae, whereas the new taxon lies at the base of the Ursinae, clearly outside either of the extant tribes. Therefore, we regard this Nebraska bear as a new genus and species (as indicated by the phylogeny in Fig. 2), as erected in the main text.

The origin of ursine bears

Bears have relatively complicated dental structures, which helps in identifying and

distinguishing their different lineages. As has been analyzed above, Early Miocene bears are rather primitive anatomically, and all appear to belong to stem lineages of Ursidae, whereas most of the Late Miocene *Ursavus* or *Ursavus*-like bears can already be placed within a tribe of extant ursine. The divergence of the two living subfamilies Ailuropodinae and Ursinae appears to date to the Middle Miocene. This phylogenetic inference is supported by recent discovery of the early ailuropodine bear *Kretzoiarctos* in the latest Middle Miocene in Spain (Abella et al., 2012).

Our analysis suggests key characters that distinguish Ursinae from Ailuropodinae and more basal groups are mostly present in the m1, corroborating the prior analysis by Jiangzuo et al. (2019). In all Ursinae, the posterior ridges of the m1 protoconid are rearranged relative to the ancestral ursid condition. In both stem Ursinae and in Ailuropodinae, there is at least one postero-lingual ridge (RPrd3), which originates from the protoconid apex and connects with the metaconid. This ridge is present more broadly in most Carnivora, and represents a primitive character. In stem ursines and Ailuropodinae this ridge is always present, and is either slightly posteriorly curved (most frequent case) or nearly straight (sometimes). The postero-buccal ridge (RPrd4) is variably present in most species of stem ursine and Ailuropodinae (Dehm, 1950; Qiu and Schmidt-Kittler, 1983), but it is always present in the only living representative of Ailuropodinae, i.e. the giant panda *Ailuropoda* (QJ, personal observation; see also Fig. 4a).

In Ursinae, there are two key innovations that are always absent in non-Ursinae species:

- 1) the RPrd3 is anteriorly curved, if this ridge is present;
- 2) the appearance of an additional posterior ridge (RPrd2).

The first character appeared in all Late Miocene “*Ursavus*” (basal ursine) species, early *Ursus* species, and all Arctotheriini (Kurten, 1966, 1967; Qiu and Qi, 1990; Tedford and Martin, 2001; Koufos, 2006; Qiu et al., 2014). In derived members of Ursini, the metaconid moved anteriorly, displacing the RPrd3 anteriorly, and eventually yielding the final loss of this ridge in later-diverging taxa (or it is weakly present and confined to the apex of the protoconid, see the example of *Ursus deningeri* in Fig. 4). All living species of *Ursus*, except *Ursus malayanus*, already lost this ridge, but this character probably evolved multiple times, as early fossil members of the Asiatic black bear *Ursus primitivus* still retains this ridge (Liu and Qiu, 2009).

The second character is present in nearly all members of Ursinae, but the form and direction of this ridge RPrd2 varies somewhat in the different lineages. In Late Miocene “*Ursavus*” species (Qiu and Qi, 1990; Koufos, 2006), the RPrd2 is always present and lingually turned to be nearly parallel with RPrd3, and is separated from the latter by a groove. This is also true for early *Ursus*, e.g. *Ursus boeckhi* from Baroth-Kopéc, Romania (Schlosser, 1899) and *Ursus rusciniensis* from Serrat d'en Vacquer (Perpignan, France) (Depéret, 1890). In later-diverging ursine bears (e.g. *Ursus minimus* and most living species), however, this ridge begins to turn buccally and connects directly with the mesoconid (Fig. 4a). In most living species, this ridge is variable in being connected with the mesoconid/mesoconid ridge or lying slightly lingual to the latter, but is never so strongly lingually turned as in the Late Miocene and early Pliocene species of

“*Ursavus*”/*Ursus*. In fossil *Tremarctos floridanus*, the RPrd2 is strongly lingually turned, as in Late Miocene “*Ursavus*” species, whereas in extant *T. ornatus*, RPrd2 tends to be smaller and indistinct (QJ, personal observation, see also Fig. S5).

In *Aurorarctos tirawa*, the first character is present in all three known m1s, and the second character is variable, being strongly developed in UNSM95213, weakly developed in UNSM95237, and absent in UNSM95224. These two characters and the phylogenetic analysis (Fig. 2) indicate that *A. tirawa* is definitely a member of Ursinae, but probably a very early representative, since the second character is still not fixed intraspecifically within this new species.

Phylogenetic matrix

The phylogenetic matrix we implement here includes 131 characters (with 130 craniodental characters and one postcranial character) and 31 taxa. We select the living wolf *Canis lupus* as the outgroup, and include all the living species of Ursidae. For fossil species of Ailuropodinae and Ursinae, we only selected relatively well-known species, since many species are represented by limited material, the characters of those other species are still poorly known, and detailed analysis of these specimens and taxa is not within the scope of this study. Nearly all species previously assigned to *Ursavus* are included in the study, to clarify the evolutionary position of *Aurorarctos tirawa*, except *Ursavus pawniensis* and *Ursavus intermedius* (represented by limited and poorly preserved material). Given the outcome of our phylogenetic analysis, showing polyphyly of “*Ursavus*”, future study of those two species should focus on whether or not they are closely related to the genotype species (and thus could continue to be considered species of *Ursavus*) or if they also should be referred to as “*Ursavus*” pending a full taxonomic study and revision of all the species previously assigned to this genus. The content of the character matrix is presented Data S1 and S2.

Phylogenetic analysis

For the Ursini, we apply the topological constraint for the relationship of living species of *Ursus* as (*Ursus thibetanus*, (*Ursus malayanus*, *Ursus ursinus*))(*Ursus americanus*, (*Ursus arctos*, *Ursus maritimus*)), since this topological has been independently documented by both genome-wide phylogeny (Kumar et al., 2017) and transposable element insertions phylogeny (Lammers et al., 2017).

The maximum parsimony analysis using TNT1.5 and without applying any topological constraints yields six equally parsimony trees. For the strict consensus tree and bootstrap values see Fig. S6. Interrelationships of the living species of *Ursus* in the unconstrained tree are not well resolved. The topologically constrained parsimony analysis yields four equally parsimony trees. For the strict consensus tree and bootstrap values of constrained analysis see Fig. S7. The Bayes Inference analyses using Mrbayes3.2.6 were set to two chains, replicated 10 million times, and with a burnin of 0.25. The final divergence of the two trains is 0.003566 for the constraint analysis and

0.0047 for the unconstrained analysis.

Both constrained and unconstrained BI analyses yield similar topologies to the maximum parsimony tree, each supporting *Aurorarctos tirawa* as the earliest stem Ursinae. The clade of *Aurorarctos tirawa* plus other members of Ursinae is supported by five characters: apex of the P4 hypocone located posterior to the paracone apex, presence of m1 protoconid posterior ridge (RPrd2), anteriorly curved m1 protoconid postero-lingual ridge, sagittally oriented m1 metaconid posterior ridge (RMed2), and presence of weak m1 hypoconid postero-medial groove. The clade representing all other members of Ursinae are more anatomically derived than *Aurorarctos tirawa* in 10 characters: p2 single-rooted; anterior and posterior notches of the P4 inner lobe indistinct; antero-lingual ridge of the P4 paracone (RPr3) indistinct; rounded M1 lingual border; M1 protocone subdivided; posterior border of m1 metaconid located at posterior border of mesoconid; presence of m1 anterior accessory cusps of entoconid; presence of m2 postero-medial ridge of protocone (RPrd2.2); presence of ridge-like m2 RHyd3; and uniform height of the mandibular horizontal ramus. This suggests that *Aurorarctos tirawa* is much less derived than both living ursines and the late Miocene taxa previously considered to represent “*Ursavus*”.

“*Ursavus*” *primaevus* is identified as the earliest diverging species of Ailuropodinae in the MP analyses, but is a slightly later-diverging member (relative to *Kretzoiarctos*) in the BI analyses. As for the contrast result, we suppose the result of MP tree probably represents the really evolutionary history from morphological and chronological aspects, since it doesn't process the P4 parastyle, which is shared by all other members of Ailuropodinae. “*Ursavus*” *primaevus* slightly more closely resembles *Miomaci* in having a relatively elongated M2 talon. The sister group of “*Ursavus*” *primaevus* and other members of Ailuropodinae of the MP tree is supported by five characters: the presence of a small M1 metastyle; M1 protocone subdivided; M2 protocone subdivided; posterior ridge of M2 protocone (postprotocrista) not strongly buccally turned; and presence of m1 RPrd4. The phylogenetic position of the type species of *Ursavus*, *U. brevirohinus*, within Ursidae is not definitive, as it falls within an unresolved polytomy with Ailuropodinae and Ursinae (Fig. 2). Since it does not possess any character unique to either subfamily, and given its placement in Fig. 2, we currently regard it as a stem group of Ursidae; future work may resolve whether it is definitively basal to other ursids or might link instead to either the ailuropodine or ursine clades. The genus *Ursavus* as traditionally conceived is clearly polyphyletic, however, representing a taxonomic wastebasket of stem ursid, stem ailuropodine, and early diverging ursine taxa. Nevertheless, we are not naming new genera for most of the various lineages represented by these bears, other than *Aurorarctos tirawa* studied intensively herein, pending a thorough systematic review of relevant European material and all taxa previously assigned to “*Ursavus*”.

Geometric morphometric analyses

To better understand the paleoecology of *Aurorarctos tirawa*, we assembled two data sets: mandible and distal humerus. For the mandible, we chose the Caniformia taxa

(with the museum repository for material studies) for comparisons in Data S3.

After Generalized Procrustes Superimposition (Rohlf and Slice, 1990), we performed principal components analyses (Adams and Otárola-Castillo, 2013) for three types of information: diet (Fig. S9), Ursinae species (Fig. S10), and Caniformia family assignment (Fig. S11). Diet is classified as carnivorous, insectivorous omnivorous, herbivorous omnivorous, and herbivorous. Carnivorous species include *Gulo gulo*, *Canis lupus*, and the extinct Hemicyoninae, all of which have enlarged carnassials (Frick, 1926; Ginsburg and Morales, 1998; Hunt 1998). There are very few Carnivora and no caniforms that prey purely on insects (the insectivorous aardwolf, *Proteles cristata*, does specialize to prey on one or two types of insect)(Kruuk and Sands, 1972). So our broader insectivorous-omnivorous suite of taxa, with piercing-cusped dentitions and non-insect items comprising a substantial part of their diets, includes *Meles* spp., *Arctonyx* spp. *Procyon lotor*, *Nasua nasua*, *Lycalopex vetulus* and *Otocyon megalotis*. *Meles* has been observed to heavily rely on insects and earthworms, but also consumed a significant amount of small vertebrates and plants (Roper and Mickevicius, 1995; Stynder and Kupczik, 2013). Similarly, *Arctonyx* also relies on insects, earthworms and plants, but earthworms are more frequently consumed and vertebrates are less common. Both *Lycalopex vetulus* and *Otocyon megalotis* consume substantial amounts of insects and fruits, dominated by insects (Kuntzsch and Nel, 1992; Stuart et al., 2003; Dalponte, 2009). *Nasua nasua* consumes both insects and fruits (Alves-Costa et al., 2004). *Procyon lotor* has a more diverse diet, but insects are often an important component (Lotze and Anderson, 1979).

The stem ursid *Ballusia* (pale blue circle, #19) falls within the variation of carnivorous and insectivorous groups. These two dietary groups generally have a slender mandible, long c-m1 distance, and short post-m1 length. The stem ursine *Aurorarctos tirawa* (large green circle, #69), on the other hand, just falls within the variation of herbivorous and herbivorous omnivorous groups, representing a dietary shift from the ancestral more insectivorous diet to a more herbivorous diet. The later-diverging fossil ursine "*Ursavus*" *tedfordi* (small green circles, #67-68) is closer to Ursinae taxa, representing a further stage towards an herbivorous omnivorous food habitat. Among the different extant Ursinae species, *Aurorarctos tirawa* is closest to *Ursus arctos*, *Ursus thibetanus* and *Ursus americanus* (Fig. S9, A10). These three species have flexible diets, but generally dominated by plants. *Ursus malayanus* and *Ursus ursinus* are specialised in having very deep mandibles, especially at the symphysis. When comparing morphology across different caniform families, *Aurorarctos tirawa* falls within the variation of extant Ursidae but outside the variation of the rest of the families within the crown group of Caniformia, but is closest to some Mustelidae (e.g., #38) and some Procyonidae (e.g., #146-148) among those other families (Fig. S11).

For postcranial comparisons, we include the several taxa (and preserved museum in the following) for comparison (both Caniformia and Feliformia were assessed, since postcrania may carry less phylogenetic signal) in Data S4.

For the postcranial data set we performed principal components analyses for three

types of information: habitat (Fig. S12, 13), Ursinae species (Fig. S14), and Carnivora family assignment (Fig. S15). The habitat is classified as four groups: arboreal, scansorial, terrestrial, or cursorial. All living bears were classified in the scansorial group, though many small-sized species, especially *Tremarctos ornatus* and *Ursus malayanus*, retain substantial ability to climb trees and frequently do so (Peyton, 1980; Fitzgerald and Krausman, 2002). The three badgers were classified in the fossorial group. *Nasua nasua*, *Ailurus fulgens*, *Arctictis binturong* and *Leopardus pardalis* were classified in the arboreal group. All canids were classified as cursorial. The wolverine *Gulo gulo* was classified in the terrestrial group.

The PCA analysis shows that *Aurorarctos tirawa* falls among the variation represented by the arboreal and non-ursid scansorial taxa (Fig. S12). However, *Aurorarctos tirawa* is more likely to be arboreal than scansorial, as the ectepicondyle of the humerus is not so expanded as in extant fossorial taxa, including all living bears and badgers (Fig. S13), and the shaft is also more slender. The development of both traits is closer to that of arboreal carnivores, e.g. *Nasua nasua* and *Arctictis binturong*. The more extended deltoid tuberosity and more pronounced undulation of the proximal margin of the distal condyle is more characteristic of Ursidae.

Different extant bear species occupy a similar ecomorphospace. *Ailuropoda*, *Tremarctos* and *Ursus thibetanus* are closer to the space occupied by arboreal carnivoran species, while other bears are more or less mixed together (Fig. S14). It is noteworthy that the stem ursid *Aurorarctos tirawa* (large green circle, #83, Fig. S15) is not close to any species of living bear, but falls within the broad range of variation of Mustelidae, and is close to some Procyonidae/Ailuridae, Felidae, and Viverridae (Fig. S15).

Dietary specialisation in Ailuropodinae

This paper explains how Ursinae bears break the ecological constraint with derived dental traits. Another subfamily of bear, Ailuropodinae, however, also has members with a plant-dominated diet that grow significantly over 20 kg. Our phylogeny suggests that Ailuropodinae include living giant panda and its ancestor *Ailurarctos*, the large *Indarctos* and several *Ursavus* or *Ursavus*-like bear. Among these taxa, only *Indarctos* and *Ailuropoda* have a relatively large body mass. *Indarctos* has enlarged P4 with large parastyle, and isotopic evidence suggests it is largely a carnivorous bear (Domingo et al., 2016). Especially, the younger members of *Indarctos*, e.g. *Indarctos zdanskyi*, tend to have a larger body size, in accordance with its increasing carnivorous dental traits (larger upper carnassial P4 and shorter M2) (Qiu and Tedford, 2003).

The giant panda is the only non-ursine Carnivora that has a body mass significantly over 20 kg while retaining a plant-dominated diet. In fact, the giant panda has a great number of specialised traits for its special diet, e.g. large and extremely heavy skull with high sagittal crest, highly complicated dental cusps and ridges, and enlarged radial sesamoid in carpal (Davis, 1964; Endo et al., 1999; Jiangzuo et al., 2019). Furthermore, the giant panda has an exceptionally low metabolism rate (Nie et al., 2015). These traits contribute to the success in gigantism of giant panda while retaining a plant-dominated

diet. The fossil members of giant panda, e.g. *Ailurarctos* are also herbivorous (Jiangzuo et al., 2019), never grow larger than the living panda.

An alternative explanation of body mass increase for Ursine bear is that this phenomenon is merely the Cope's rule (Stanley, 1973; Raia et al., 2012). Indeed, the living omnivorous bears generally have larger body size than those of the Middle and Late Miocene Ursinae bears. Giant panda lineage may serve as a good comparison to test if the larger body size of the Ursinae bear is merely due to their longer evolutionary history. We chose four giant panda species that are confidently herbivorous (Jiangzuo et al., 2019), and several "*Ursavus*" and *Ursus* as well as *Tremarctos* from the Late Miocene to now (Table S3) as representatives the ursine bears with plant-dominated diet. The (bisexual mean) body mass of the living species follows (Christiansen, 2007). We use a simple way to calculate the body mass for fossil species: direct cubic scale of m1 length for Quaternary species of their closest living species (e.g. *Ursus spelaeus* will be scaled to *U. arctos*, and *Tremarctos floridanus* will be scaled to *T. ornatus*), and a mean of cubic of each family for Late Miocene species, since at this period, the two subfamilies' body plans still not differ significantly. This method may not be accurate, but enough for comparison of ecological differences between the two lineages. We then plot the body mass and age.

We can see that during the Late Miocene, when Ursinae only had an initial stage of derived m1 morphology, the two lineages have similar body mass. Cope's rule generally applies to both lineages, though Ursinae, with its gradually evolved m1 structure, significantly increases the body mass than the giant panda lineage does. This suggests that Cope's rule along, can not explain the successful gigantism of Ursinae.

Appendix References

- Abella, J., Alba, D.M., Robles, J.M., Valenciano, A., Rotgers, C., Carmona, R., Montoya, P., Morales, J., 2012. *Kretzoiarctos* gen. nov., the oldest member of the giant panda clade. PLoS ONE 7, 1-7.
- Adams, D.C., Otárola-Castillo, E., 2013. geomorph: an R package for the collection and analysis of geometric morphometric shape data. *Methods in Ecology and Evolution* 4, 393-399.
- Alves-Costa, C.P., Da Fonseca, G.A., Christófaro, C., 2004. Variation in the diet of the brown-nosed coati (*Nasua nasua*) in southeastern Brazil. *Journal of Mammalogy* 85, 478-482.
- Bapst, D.W., 2012. paleotree: an R package for paleontological and phylogenetic analyses of evolution. *Methods in Ecology & Evolution* 3, 803-807.
- Christiansen, P., 2007. Evolutionary implications of bite mechanics and feeding ecology in bears. *Journal of Zoology* 272, 423-443.
- Crusafont Pairó, M., Kurtén, B., 1976. Bears and bear-dogs from the Vallesian of the Vallés-Penedés basin, Spain. *Acta Zoologica Fennica* 144, 1-30.
- Dalponte, J.C., 2009. *Lycalopex vetulus* (Carnivora: Canidae). *Mammalian Species*, 1-7.
- Davis, D.D., 1964. The giant panda: a morphological study of evolutionary mechanisms. Chicago Natural History Museum, Fieldiana: Zoology memoirs, 3, Chicago.
- Dehm, R., 1950. Die Raubtiere aus dem Mittel-Miocän (Burdigalium) von Wintershof-West bei Eichstätt in Bayern. *Bayerische Akademie der Wissenschaften, Abhandlungen* 58.

- Depéret, C., 1890. Animaux Pliocènes du Roussillon. Mémoires de la Société Géologique de France, Paléontologie 1, 1-88.
- Domingo, M.S., Domingo, L., Abella, J., Valenciano, A., Badgley, C., Morales, J., 2016. Feeding ecology and habitat preferences of top predators from two Miocene carnivore-rich assemblages. *Paleobiology* 42, 489-507.
- Endo, H., Yamagiwa, D., Hayashi, Y., Koie, H., Yamaya, Y., Kimura, J., 1999. Role of the giant panda's 'pseudo-thumb'. *Nature* 397, 309-310.
- Fitzgerald, C.S., Krausman, P.R., 2002. *Helarctos malayanus*. Mammalian Species, 1-5.
- Frick, C., 1926. The Hemicyoninae and an American Tertiary bear. Bulletin of the AMNH 56, 1883-1965.
- Gaillard, C., 1899. Mammifères miocènes nouveaux ou peu connus de La Grive-Saint-Alban (Isère). Archives du Muséum d'histoire naturelle de Lyon 7, 1-77.
- Ginsburg, L., Morales, J., 1998. Les Hemicyoninae (Ursidae, Carnivora, Mammalia) et les formes apparentées du Miocène inférieur et moyen d'Europe occidentale. *Annales de Paléontologie* 84, 71-123.
- Goloboff, P.A., Catalano, S.A., 2016. TNT version 1.5, including a full implementation of phylogenetic morphometrics. *Cladistics* 32, 221-238.
- Goloboff, P.A., Farris, J.S., Nixon, K.C., 2008. TNT, a free program for phylogenetic analysis. *Cladistics* 24, 774-786.
- Hofmann, A., 1887. Über einige Saugethierreste aus der Braunkohle von Voitsberg und Steieregg bei Wies. Steiermark, Jb. KK Geol. Reichsanstalt. Wien 37, 207-217.
- Hofmann, A., 1892. Beiträge zur miozänen Säugethierfauna der Steiermark. Jahrbuch der Kaiserlich Königlich Geologischen Reichsanstalt 42, 63-76.
- Huelsenbeck, J.P., Ronquist, F., 2001. MRBAYES: Bayesian inference of phylogenetic trees. *Bioinformatics* 2001, 754-755.
- Hunt, R.M., JR, 1998. 10 Ursidae, in: Janis, C.M., Scott, K.M., Jacobs, L.L. (Eds.), *Evolution of Tertiary Mammals of North America: Terrestrial carnivores, ungulates, and ungulate-like mammals*. Cambridge University Press, pp. 174-195.
- Jiangzuo, Q., Liu, J., Chen, J., 2019. Morphological homology, evolution and proposed nomenclature for bear dentition. *Acta Palaeontologica Polonica*.
- Koufos, G.D., 2006. The late Miocene Vertebrate locality of Perivolaki, Thessaly, Greece. 4. Carnivora. *Palaeontographica, Abt. A* 276, 39-74.
- Kretzoi, M., 1942. Zwei neue Agriotheriiden aus dem ungarischen Pannon[J]. *Foldtani Kozlony. Foldtani Kozlony* 72, 350-353.
- Kruuk, H., Sands, W., 1972. The aardwolf (*Proteles cristatus* Sparman) 1783 as predator of termites. *African Journal of Ecology* 10, 211-227.
- Kumar, V., Lammers, F., Bidon, T., Pfenninger, M., Kolter, L., Nilsson, M.A., Janke, A., 2017. The evolutionary history of bears is characterized by gene flow across species. *Scientific Report* 7: 46487 1-10.
- Kuntzsch, V., Nel, J., 1992. Diet of bat-eared foxes *Otocyon megalotis* in the Karoo. *Koedoe* 35, 37-48.
- Kurten, B., 1966. Pleistocene bears of North America. 1. Genus *Tremarctos*, spectacled bears. . *Acta Zoologica Fennica* 115, 1-120.
- Kurten, B., 1967. Pleistocene bears of North America: 2 genus *Arctodus*, short faced bears. *Acta*

- Zoologica Fennica 117, 1–60.
- Lammers, F., Gallus, S., Janke, A., Nilsson, M.A., 2017. Phylogenetic conflict in bears identified by automated discovery of transposable element insertions in low-coverage genomes. *Genome Biology and Evolution* 9, 2862-2878.
- Liu, J.Y., Qiu, Z.X., 2009. Mammalian-Carnivora in: Jin, C.Z., Liu, J.Y. (Eds.), *Palaeolithic Site-The Renzidong Cave, Fanchang, Anhui Province*. Science Press, Beijing, pp. 220-282.
- Lotze, J.-H., Anderson, S., 1979. *Procyon lotor*. *Mammalian species*, 1-8.
- Muda, N., Othman, A.R., 2015. APE: analyses of phylogenetics and evolution in R language. *Aip Conference Proceedings* 20, 289-290.
- Nie, Y., Speakman, J.R., Wu, Q., Zhang, C., Hu, Y., Xia, M., Yan, L., Hambly, C., Wang, L., Wei, W., Zhang, J., Wei, F., 2015. Exceptionally low daily energy expenditure in the bamboo-eating giant panda. *Science* 349, 171-174.
- Peyton, B., 1980. Ecology, Distribution, and Food Habits of Spectacled Bears, *Tremarctos ornatus*, in Peru. *Journal of Mammalogy* 61, 639-652.
- Pinheiro, J., Bates, D., Debroy, S., Sarkar, D., Team, R.C., 2013. nlme: Linear and Nonlinear Mixed Effects Models. .
- Qi, G.Q., 1984. First discovery of *Ursavus* in China and note on other Ursidae specimens from the Ramapithecus fossil site of Lufeng. *Acta Anthropologica Sinica* 1, 53-61.
- Qiu, Z., Qi, G., 1990. Restudy of mammalian fossils referred to Ursinae Indet. from *Lufengpithecus* Locality. *Certebrata Palasiatica* 4, 270-283.
- Qiu, Z.X., Deng, T., Wang, B.Y., 2014. A Late Miocene *Ursavus* skull from Guanghe, Gansu, China. *Vertebrata PalAsiatica* 52, 265-302.
- Qiu, Z.X., Qi, G.Q., 1989. Ailuropod found from the Late Miocene deposits in Lufeng, Yunnan. *Vertebrata PalAsiatica* 27, 153-169.
- Qiu, Z.X., Schmidt-Kittler, N., 1983. *Agriotherium intermedium* (Stach 1957) from a Pliocene fissure filling of Xiaoxian County (Anhui Province, China) and the phylogenetic position of the genus. *Palaeovertebrata* 13, 65-81.
- Qiu, Z.X., Tedford, R.H., 2003. A new species of *Indarctos* from Baode, China. *Vertebrata PalAsiatica* 41, 278-288.
- Qiu, Z.X., Yan, D.F., Jia, H., Wang, B.Z., 1985. Dentition of the *Ursavus* skeleton from Shanwang, Shandong province. *Vertebrata Palasiatica* 23, 264-271.
- R Development Core Team, 2016. R: A language and environment for statistical computing. R Foundation for Statistical Computing, Vienna, Austria.
- Raia, P., Carotenuto, F., Passaro, F., Fulgione, D., Fortelius, M., 2012. Ecological specialization in fossil mammals explains Cope's rule. *The American Naturalist* 179, 328-337.
- Revell, L.J., 2012. phytools: an R package for phylogenetic comparative biology (and other things). *Methods in Ecology and Evolution* 3, 217-223.
- Rohlf, F.J., Slice, D., 1990. Extensions of the Procrustes method for the optimal superimposition of landmarks. *Systematic Biology* 39, 40-59.
- Ronquist, F., Teslenko, M., Mark, P.v.d., Ayres, D.L., Darling, A., Höhna, S., Larget, B., Liu, L., Suchard, M.A., Huelsenbeck, a.J.P., 2012. MrBayes 3.2: efficient Bayesian phylogenetic inference and model choice across a large model space. *Systematic biology* 61, 539-542.
- Roper, T., Mickevicius, E., 1995. Badger *Meles meles* diet: a review of literature from the former Soviet Union. *Mammal Review* 25, 117-129.

- Schlosser, M., 1899. Über die Bären und bärenähnlichen Formen des europäischen Tertiärs. *Palaeontographica*, A 46, 95–148.
- Stanley, S.M., 1973. An explanation for Cope's rule. *Evolution* 27, 1-26.
- Stuart, C.T., Stuart, T., Pereboom, V., 2003. Diet of the bat-eared fox (*Otocyon megalotis*), based on scat analysis, on the Western Escarpment, South Africa. *Canid News* 6, 1-5.
- Stynder, D.D., Kupczik, K., 2013. Tooth root morphology in the early Pliocene African bear *Agriotherium africanum* (Mammalia, Carnivora, Ursidae) and its implications for feeding ecology. *Journal of Mammalian Evolution* 20, 227-237.
- Tedford, R.H., Martin, J., 2001. *Plionarctos*, a tremarctine bear (Ursidae: Carnivora) from western North America. *Journal of Vertebrate Paleontology* 21, 311-321.
- Thenius, E., 1947. *Ursavus ehrenbergi* aus dem Pont von Euböa (Griechenland). *Sitz-ber Akad Wiss Wien* 156.
- Thenius, E., 1949. Beiträge zur Kenntnis der Säugetierreste des steirischen Tertiärs. 4. Die Carnivoren von Göriach (Steiermark). Springer.
- Thenius, E., 1979. Zur systematischem und phylogenetischen Stellung des Bambusbären: *Ailuropoda melanoleuca* David (Carnivora, Mammalia). *Zeitschrift für Säugetierkunde* 44, 286–305.
- Viret, J., 1949. Observations complementaires sur quelques mammiferes fossiles de Soblay[*Eclogae Geologicae Helvetiae* 42, 469-476.
- Wegner, R.N., 1913. Tertiär und umgelagerte Kreide bei Oppeln (Oberschleisien). *Paläontographica* 60, 175–274.
- Wickham, H., 2016. *ggplot2: elegant graphics for data analysis*. Springer, New York.
- Zong, G.F., 1997. 5.3.4 Carnivora, in: He, Z.Q. (Ed.), *Yuanmou Hominoid Fauna*. Yunnan Science and Technology Press, Kunming, pp. 69-88.

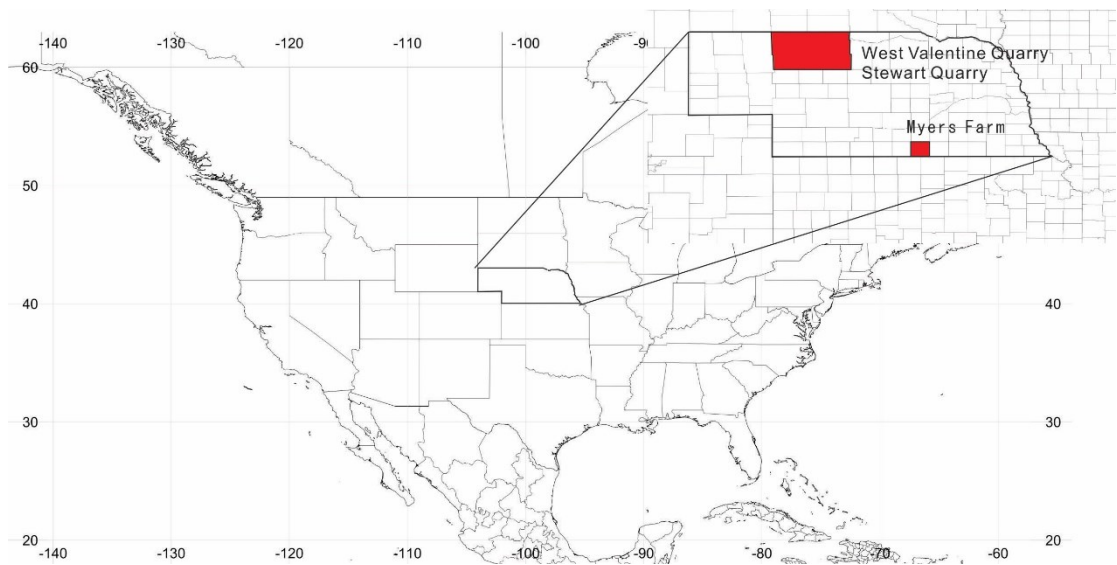


Fig. S1. Related to Fig. 2. Location of fossil localities. Background from Simplemappr: <https://www.simplemappr.net/#tabs=0>

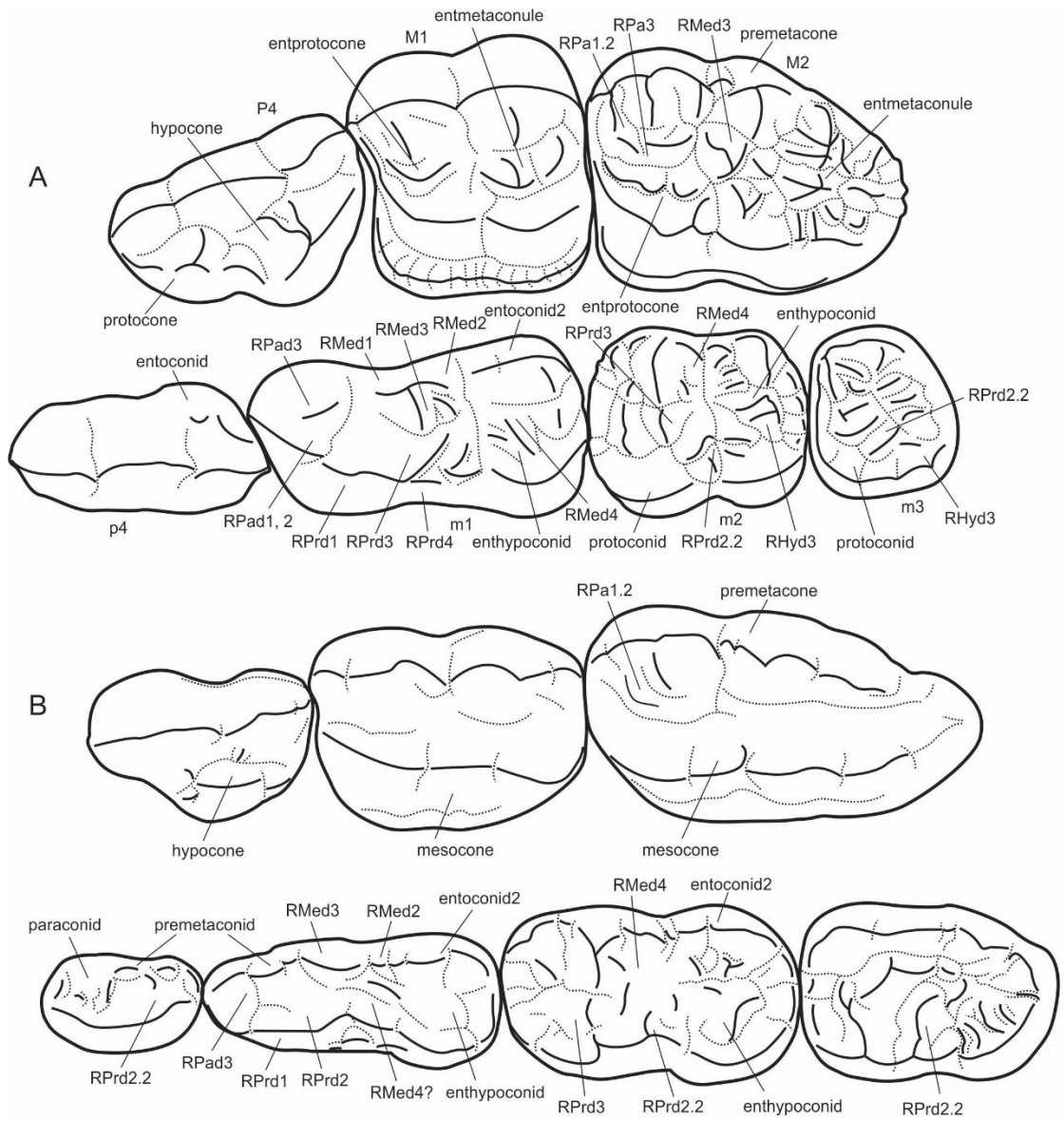


Fig. S2. Related to Fig. 1. Ursid dental terminology. a. *Ailuropoda melanoleuca*; b. *Ursus deningeri*.

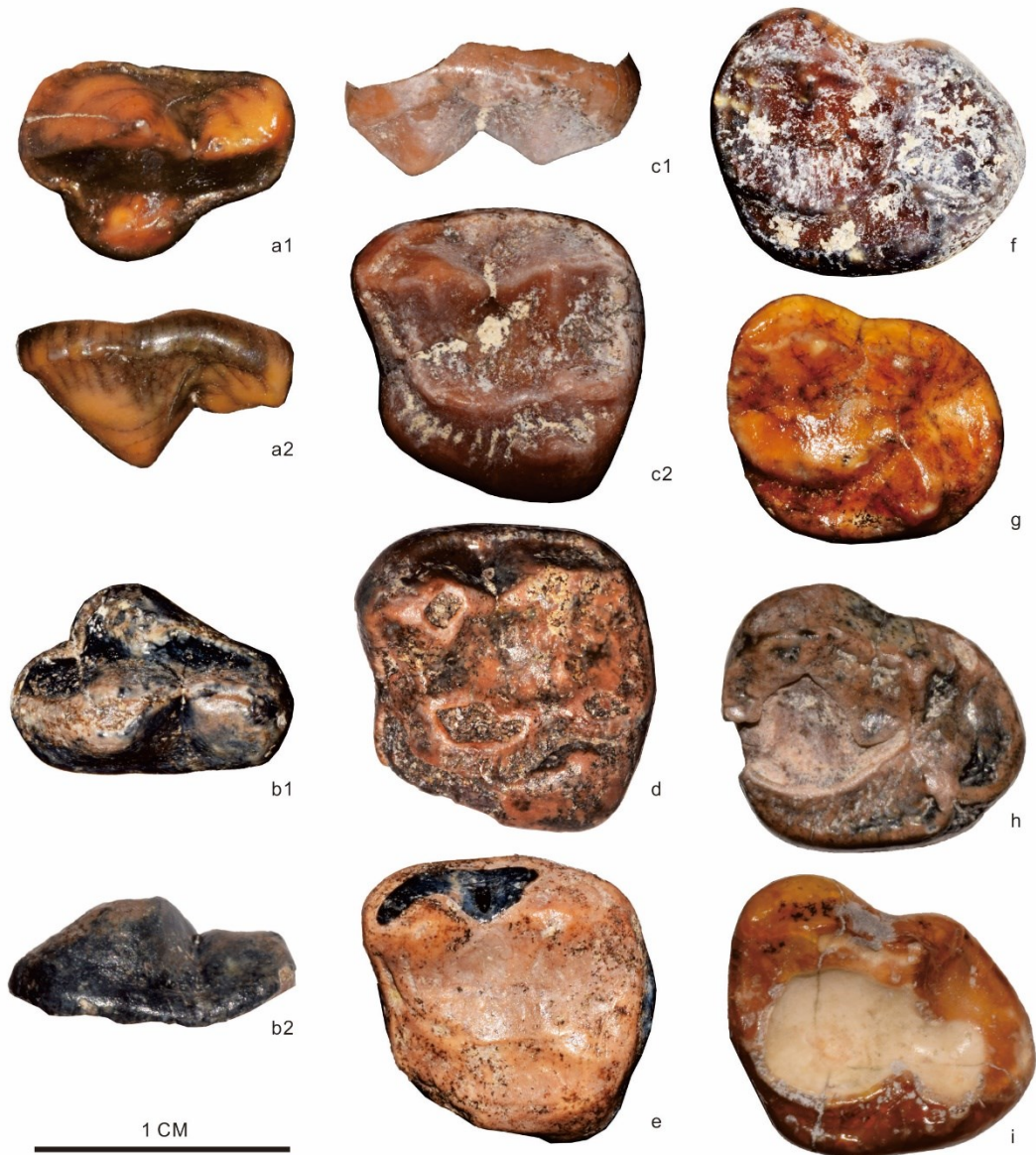


Fig. S3. Related to Fig. 1. Upper dentition of *Aurorarctos tirawa*. a1-2. UNSM95211, P4, occlusal and lateral views; b1-2. UNSM95210, P4, occlusal and lateral views; c1-2. UNSM95209, M1, lateral and occlusal views; d. UNSM95207, M1, occlusal view; e. UNSM95208, M1, occlusal view; f. UNSM95212, M2, occlusal view; g. UNSM95206, M2, occlusal view; h. UNSM95200, M2, occlusal view; i. UNSM45086, M2, occlusal view.



Fig. S4. Related to Fig. 1. Lower dentition (occlusal view) of *Aurorarctos tirawa*. A. UNSM95213, m1; B. UNSM95224, m1; C. UNSM95237, m1; D. UNSM95214, m1 fragment; E. UNSM95237, m2; F. UNSM95215, m2.

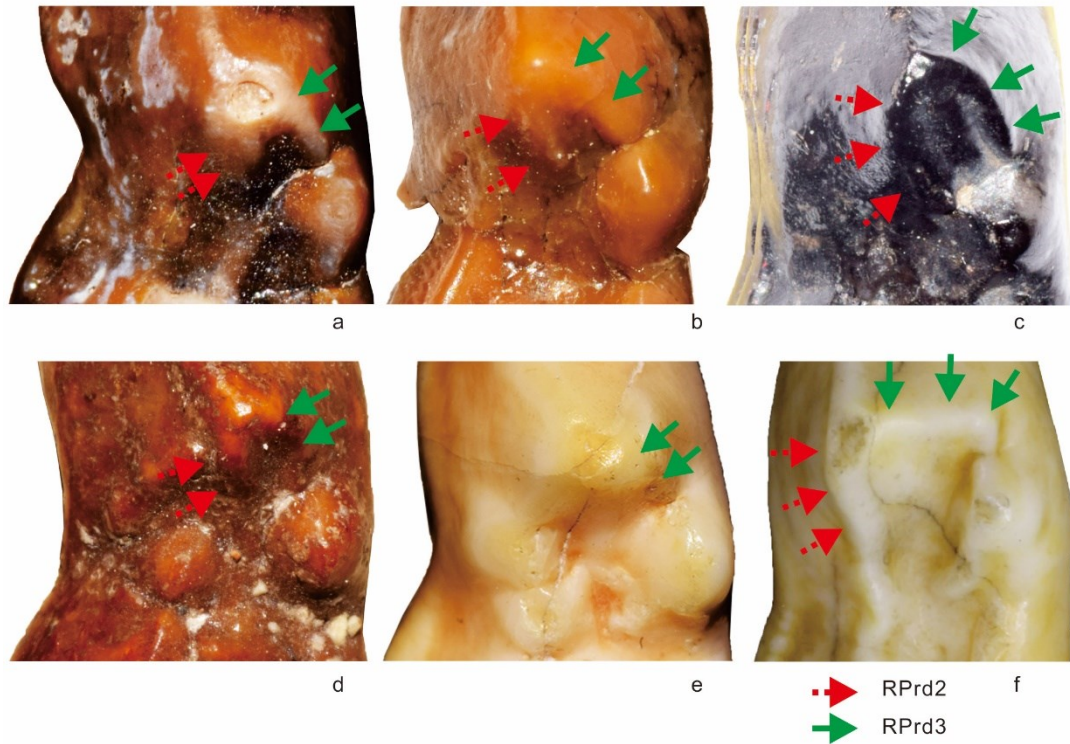


Fig. S5. Related to Fig. 5. Comparison of the protoconid region of *Aurorarctos tirawa* and related taxa. a-b *A. tirawa*, UNSM95237, UNSM95213; c. *Ursus sylvestris* from Lufeng V6894.14; d. *Tremarctos floridanus*; e. *Tremarctos ornatus* AMNH M70164; f. *Ursus malayanus* AMNH M19154.

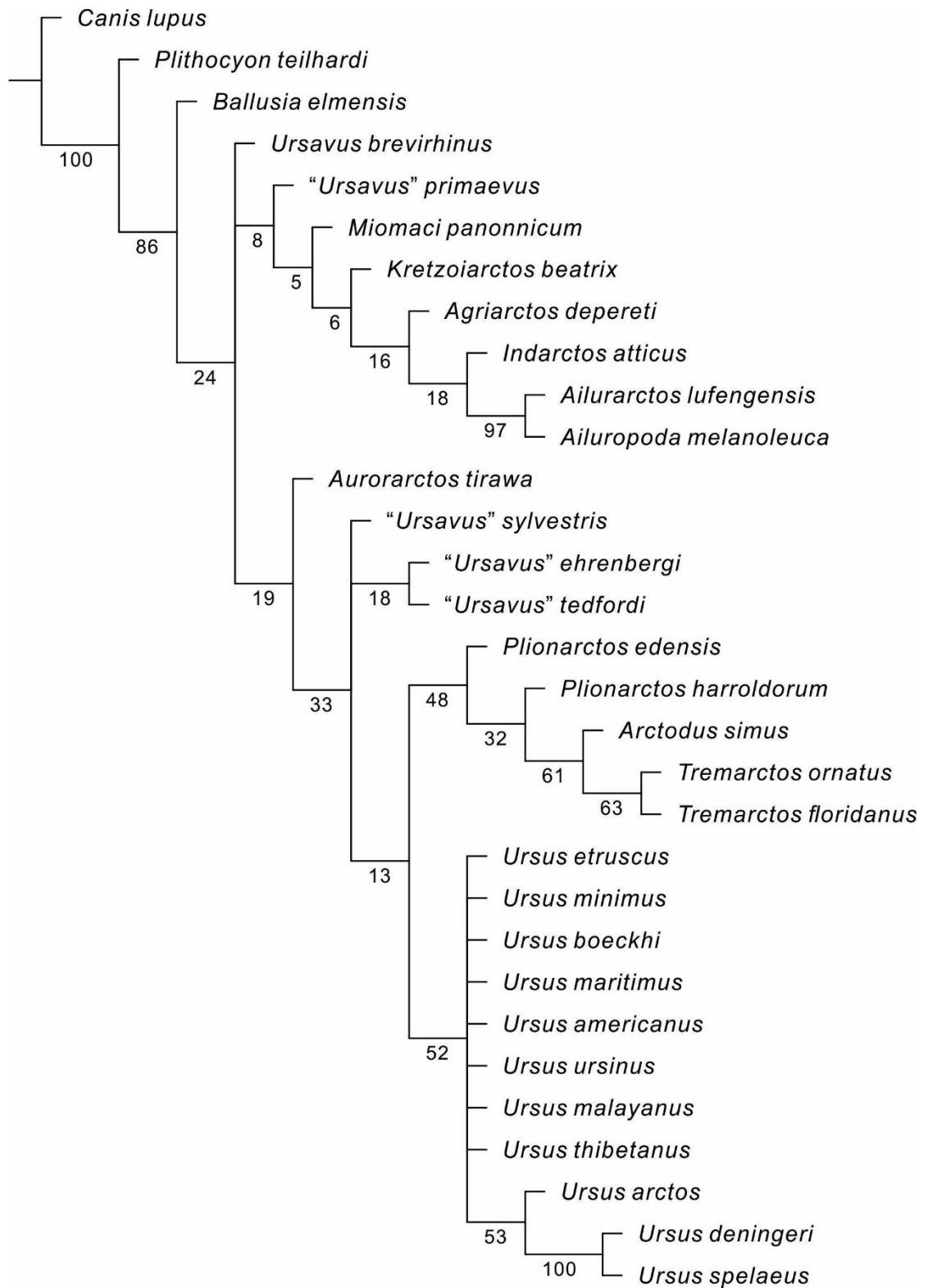


Fig. S6. Related to Fig. 3. Strict consensus MP tree of Ursidae without topological constraint. Values at nodes represent bootstrap percentages from 1000 bootstrap replicates.

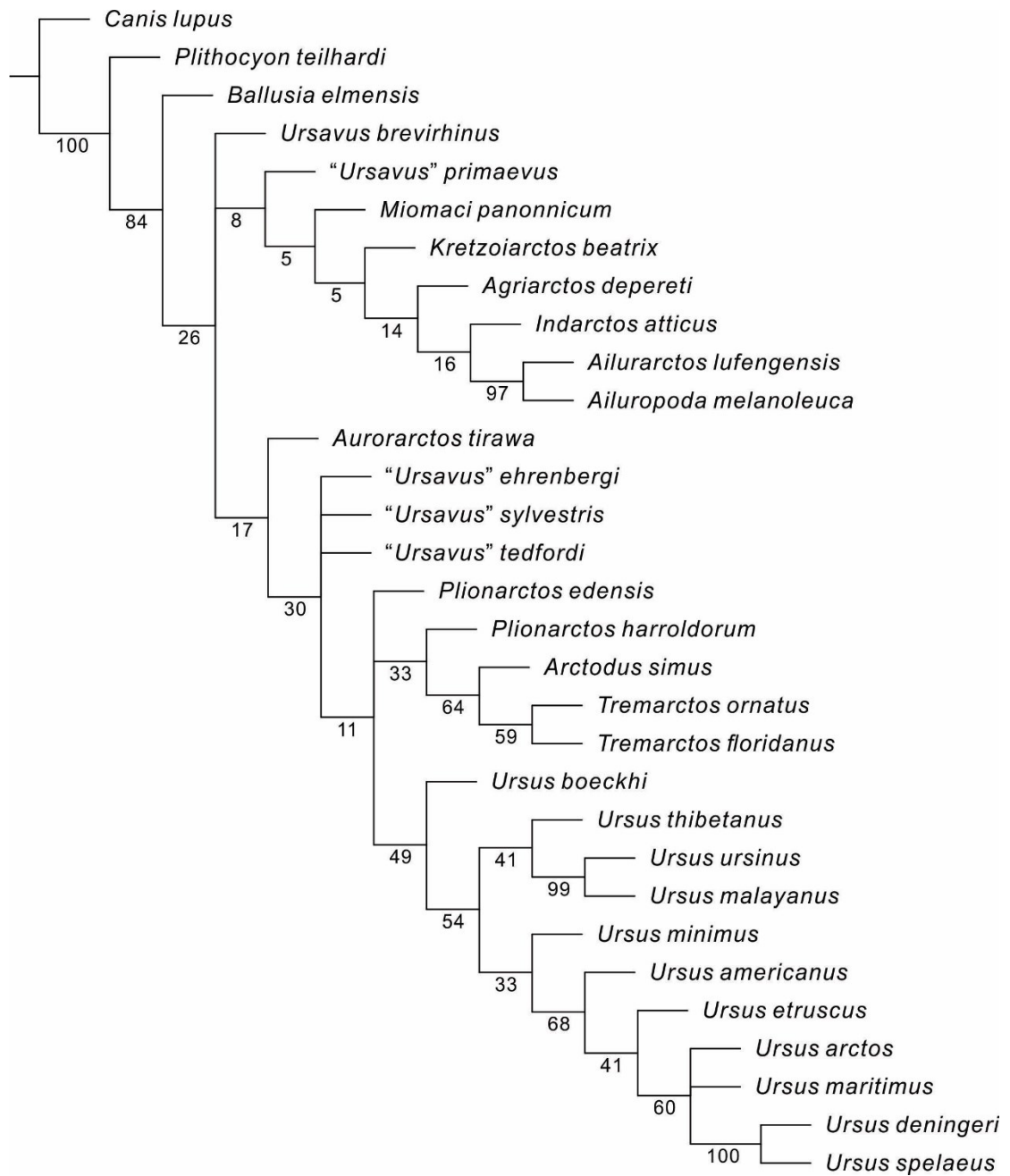


Fig. S7. Related to Fig. 3. Strict consensus MP tree of Ursidae with topological constraint (see text). Values at nodes represent bootstrap percentages from 1000 bootstrap replicates.

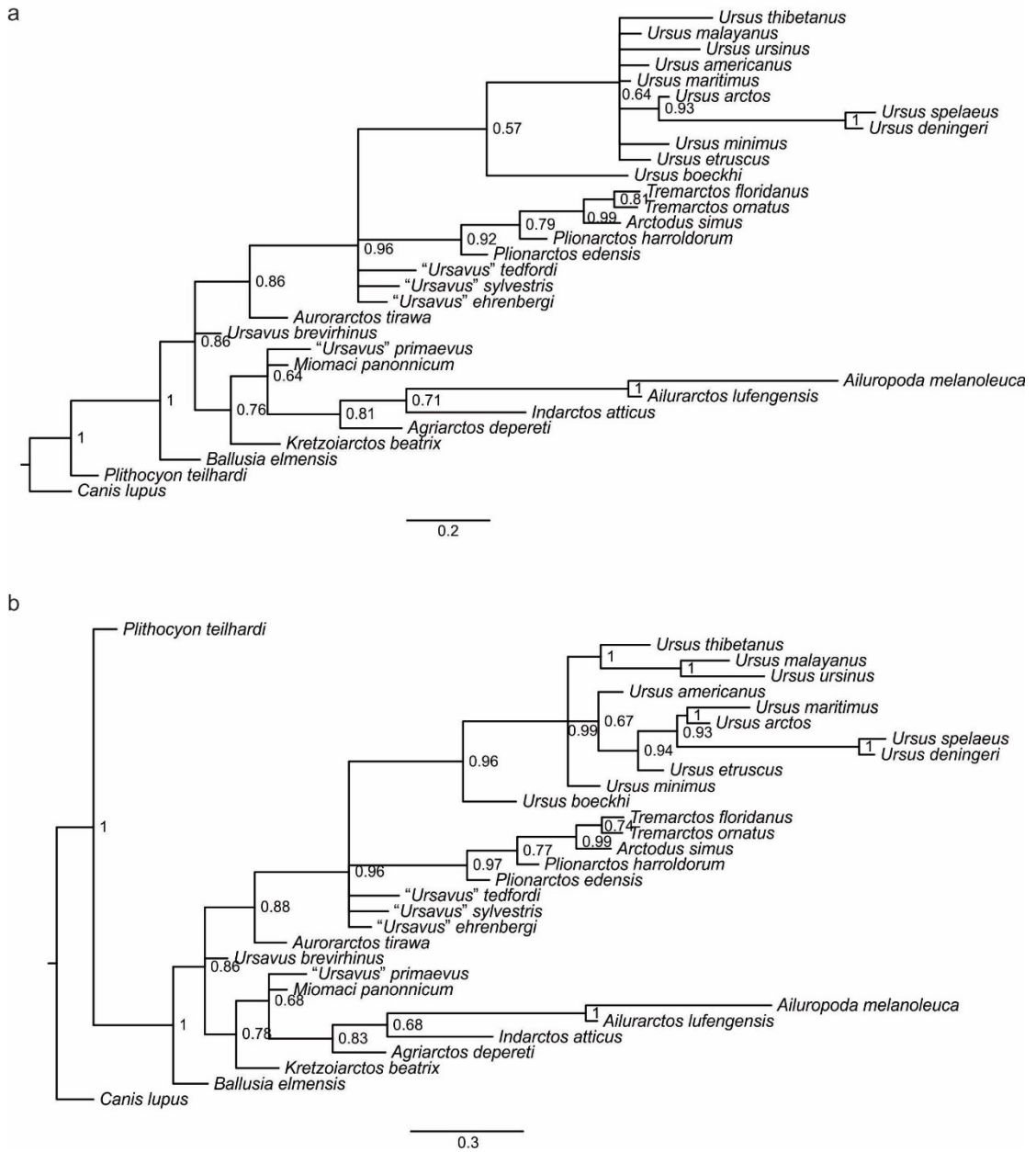


Fig. S8. Related to Fig. 3. Bayes Inference tree of Ursidae without (a) and with (b) topological constraint. Values at nodes represent posterior probability.

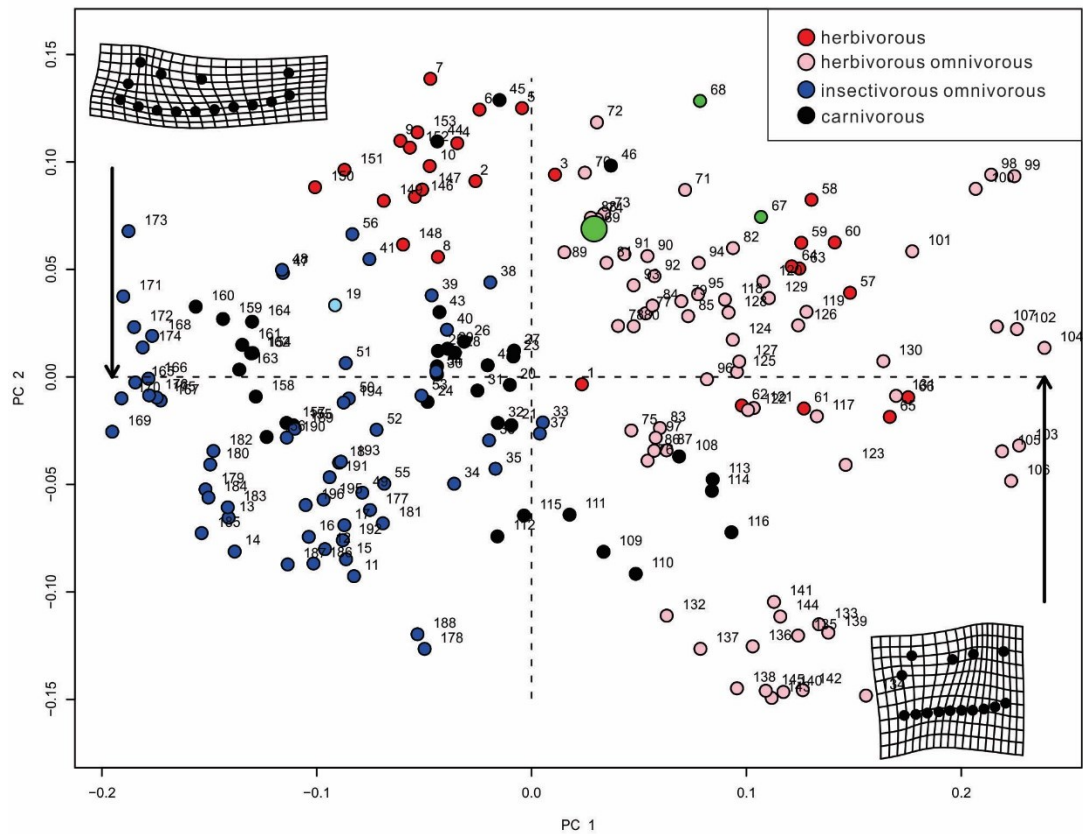


Fig. S9. Related to Fig. 4. Geometric morphometric analysis (PCA) of caniform mandibles, categorized by dietary ecology type. PC1 represents the first principal component (54.6%), and PC2 represents the second principal component (20.1%). Specimen numbers and taxa: 1–10, *Ailuropoda melanoleuca*; 11–18, *Arctonyx* spp.; 19, *Ballusia elmensis*; 20–32 *Gulo gulo*; 33–41, *Meles* spp.; 42–46 Hemicyoninae; 47–56, *Procyon lotor*; 57–66, *Tremarctos ornatus*; 67–68, “*Ursavus*” *tedfordi*; 69, *Aurorarctos tirawa* gen. et sp. nov.; 70–82, *Ursus americanus*; 83–97, *Ursus arctos*; 98–107, *Ursus malayanus*; 108–116, *Ursus maritimus*; 117–131, *Ursus thibetanus*; 132–145 *Ursus ursinus*; 146–153, *Ailurus fulgens*; 154–164, *Canis lupus*; 165–176, *Lycalopex vetulus*; 177–188, *Nasua nasua*; 189–196, *Otocyon megalotis*.

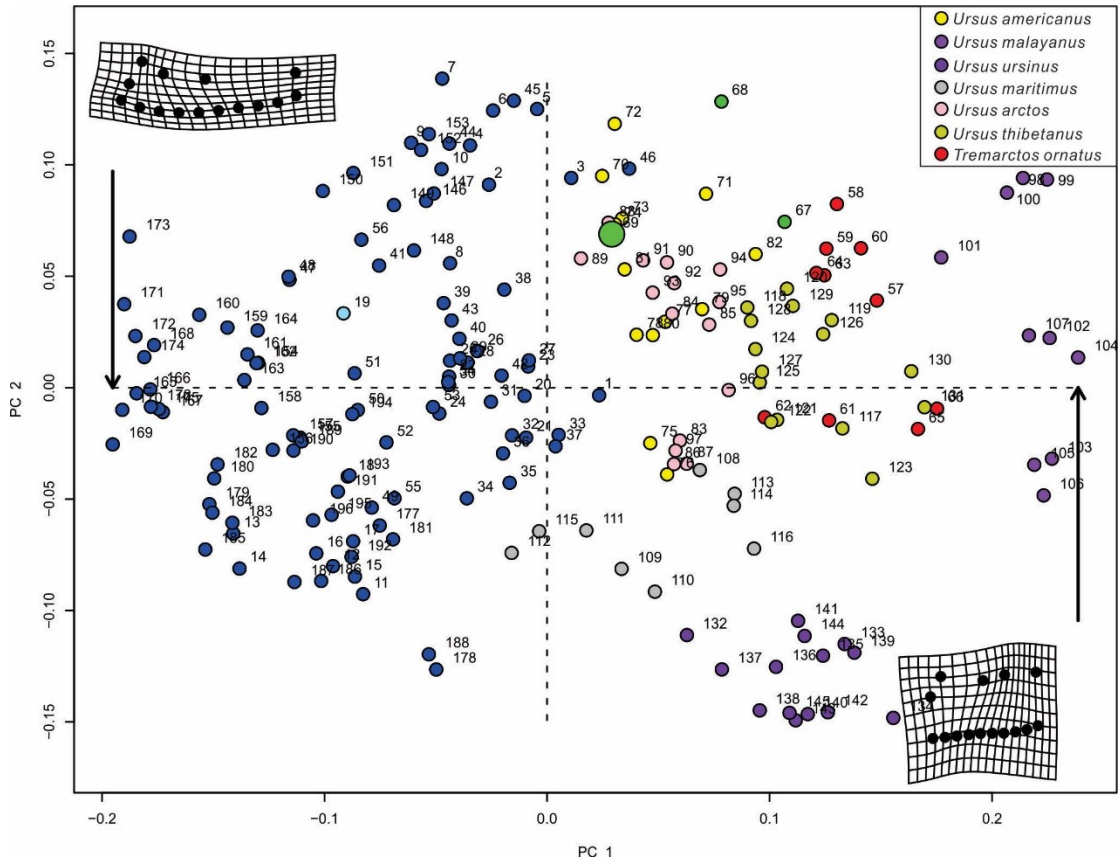


Fig. S10. Related to Fig. 4. Geometric morphometric analysis (PCA) of mandibles, categorized by Ursinae species. Specimen numbers/taxa as in Fig. S9.

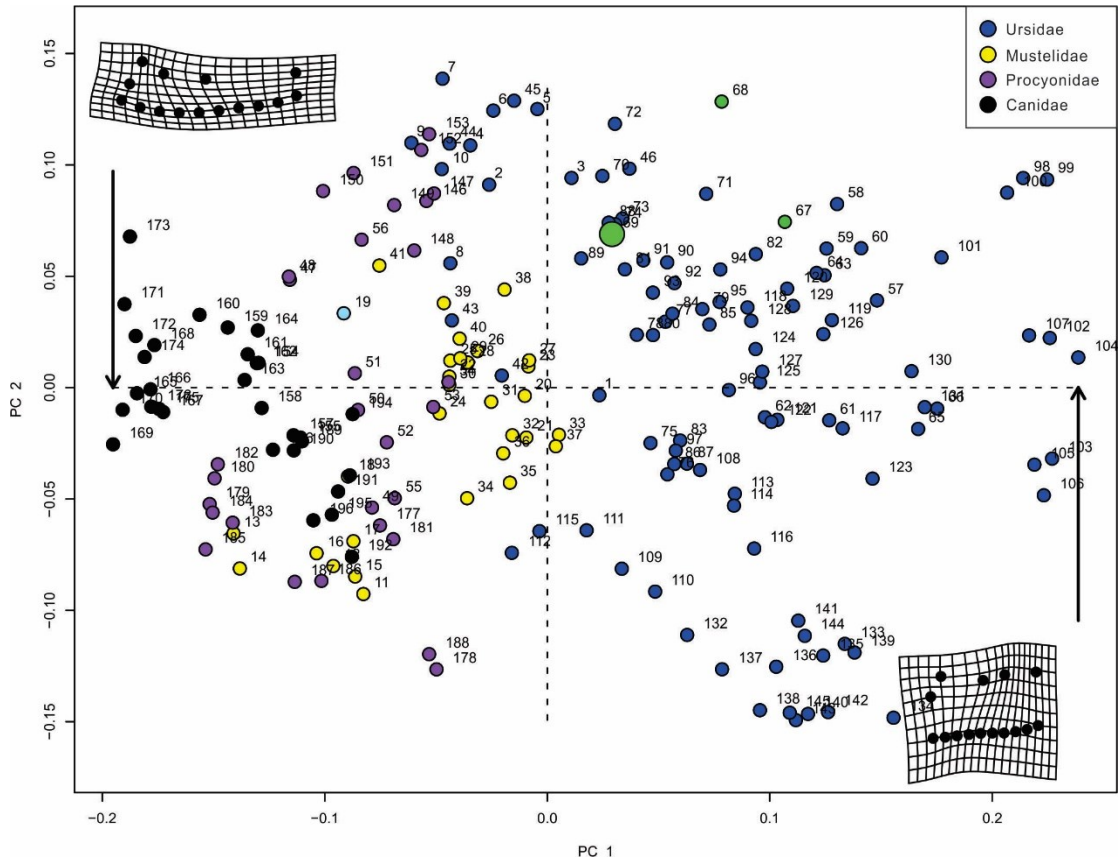


Fig. S11. Related to Fig. 4. Geometric morphometric analysis (PCA) of mandibles, categorized by family. Specimen numbers/taxa as in Fig. S9.

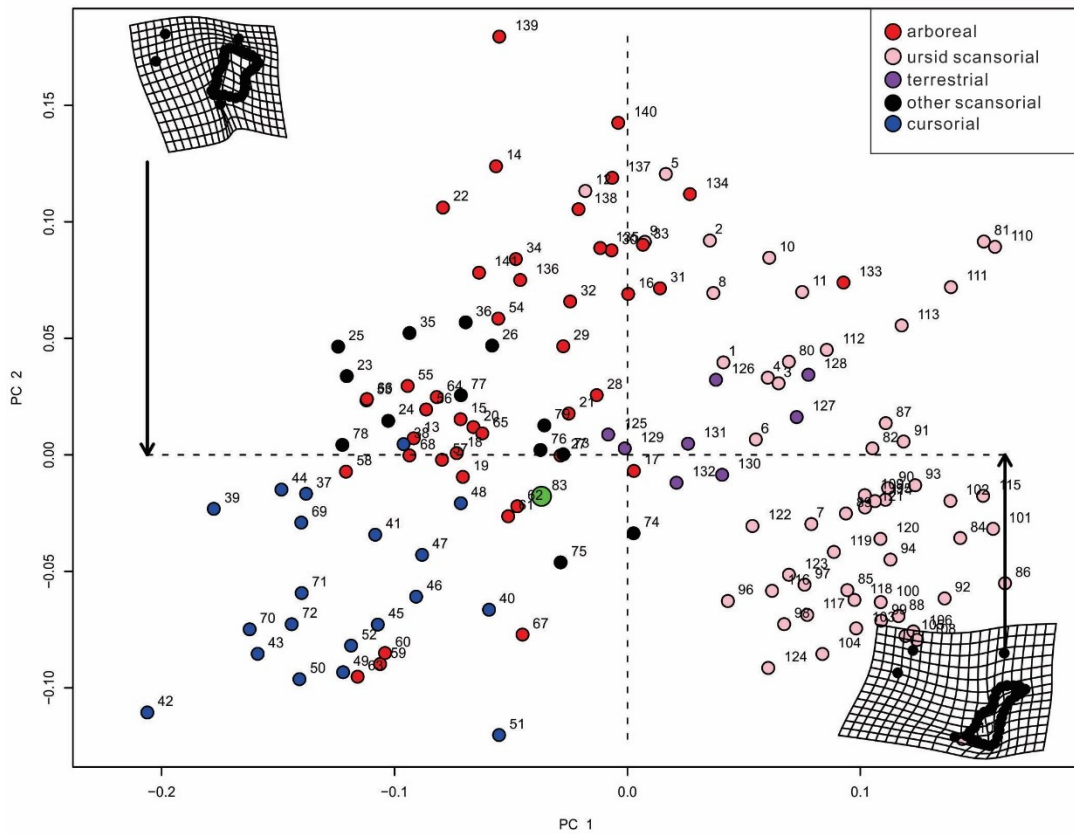


Fig. S12. Related to Fig. 4. Geometric morphometric analysis (PCA) of the distal humerus, categorized by ecological type. PC1 represents the first principal component (52.3%), and PC2 represents the second principal component (23.6%). Specimen numbers and taxa: 1–12, *Ailuropoda melanoleuca*; 13–22, *Ailurus fulgens*; 23–26, *Meles* spp.; 27–34, *Arctictis binturong*; 35–36, *Arctonyx* spp.; 37–44, *Canis adustus*; 45–52, *Canis lupus*; 53–60, *Civettictis civetta*; 61–68, *Leopardus pardalis*; 69–72, *Lycalopex vetulus*; 73–79, *Taxidea taxus*; 80–82, *Tremarctos ornatus*; 83, *Aurorarctos tirawa*; 84–90, *Ursus americanus*; 91–100, *Ursus arctos*; 101–103, *Ursus malayanus*; 104–108, *Ursus maritimus*; 109–115, *Ursus thibetanus*; 116–124, *Ursus ursinus*; 125–132, *Gulo gulo*; 133–141, *Nasua nasua*.

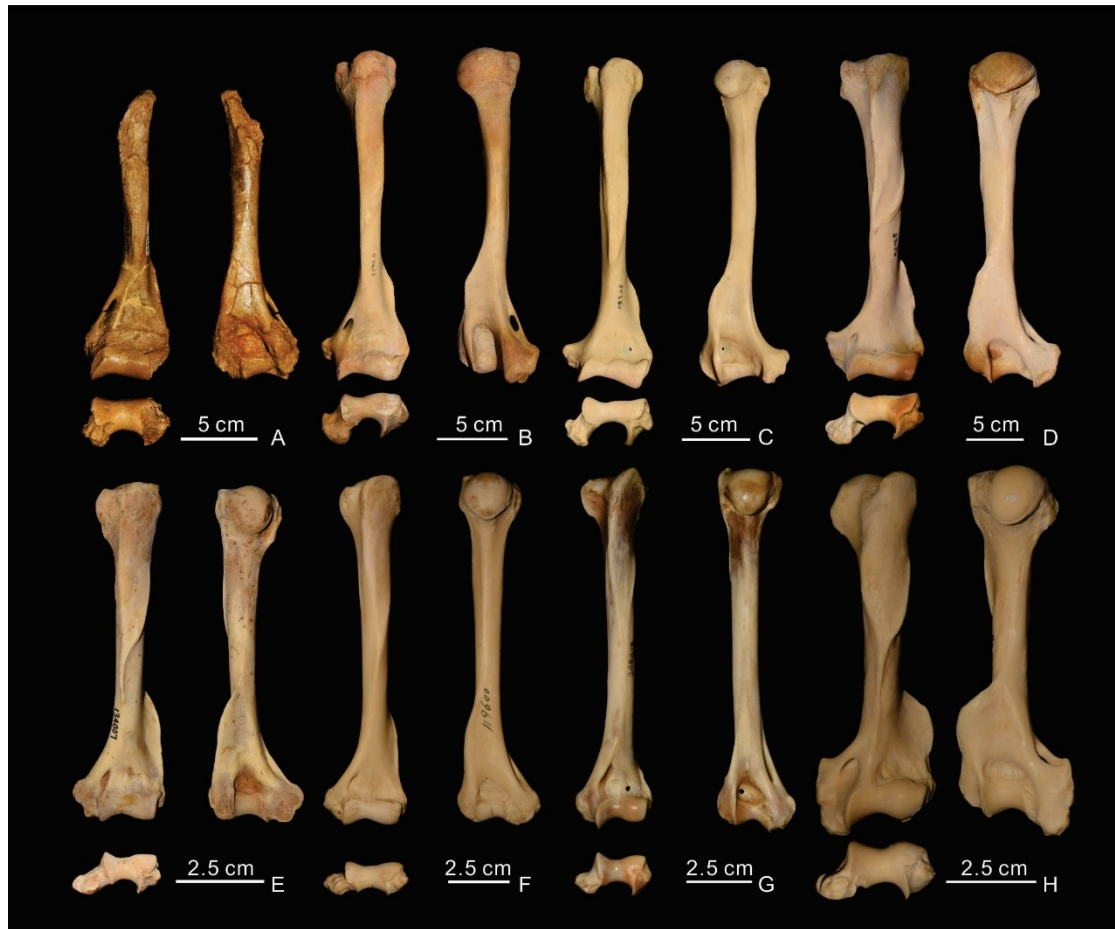


Fig. S13. Related to Fig. 4. Comparison of the humerus of *Aurorarctos tirawa* to selected other arboreal/scansorial taxa. A. UNSM45118 *Aurorarctos tirawa*; B. AMNH M35440 *Tremarctos ornatus*; C. AMNH M35864 *Ursus malayanus*; D. AMNH M89028 *Ailuropoda melanoleuca*; E. AMNH M134007 *Nasua nasua*; F. AMNH M119600 *Arctictis binturong*; G. AMNH M248728 *Leopardus pardalis*; H. AMNH M171360 *Taxidea taxus*. All specimens are adjusted to the same length for comparison.

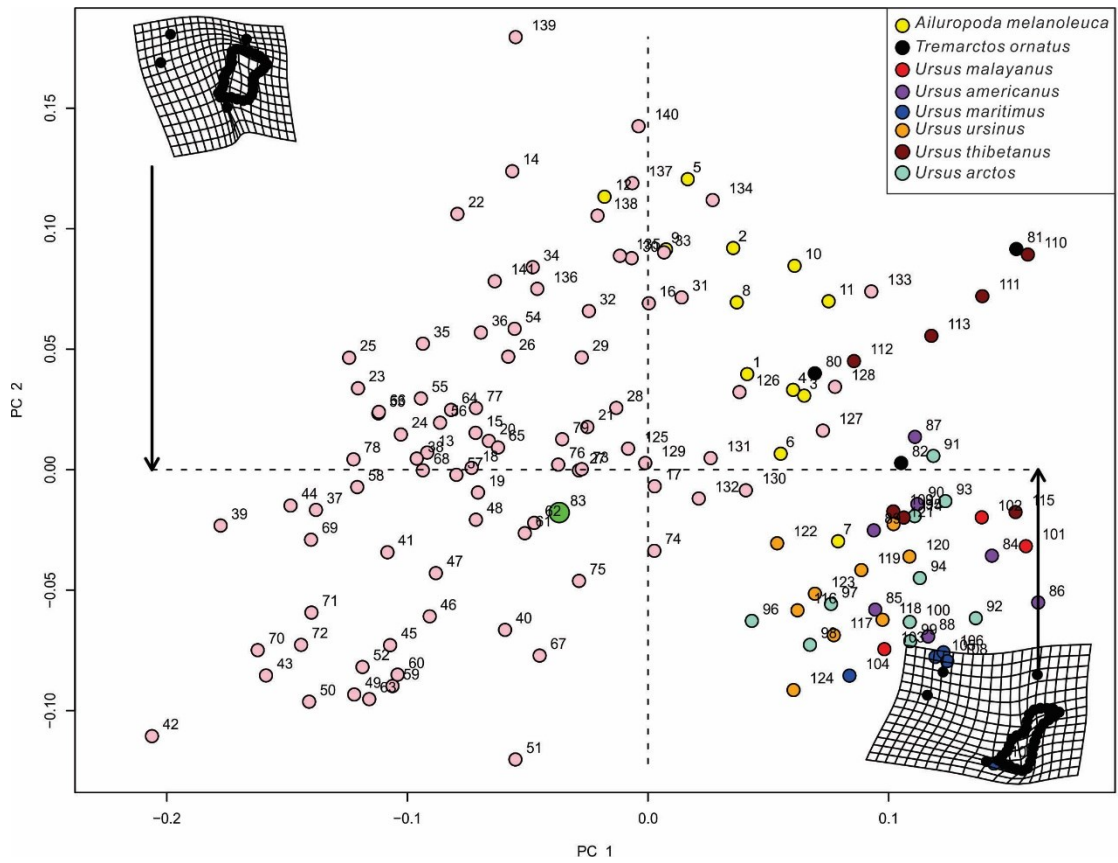


Fig. S14. Related to Fig. 4. Geometric morphometric analysis (PCA) of the distal humerus, categorized by the species of extant bear. Specimen numbers/taxa as in Fig. S12.

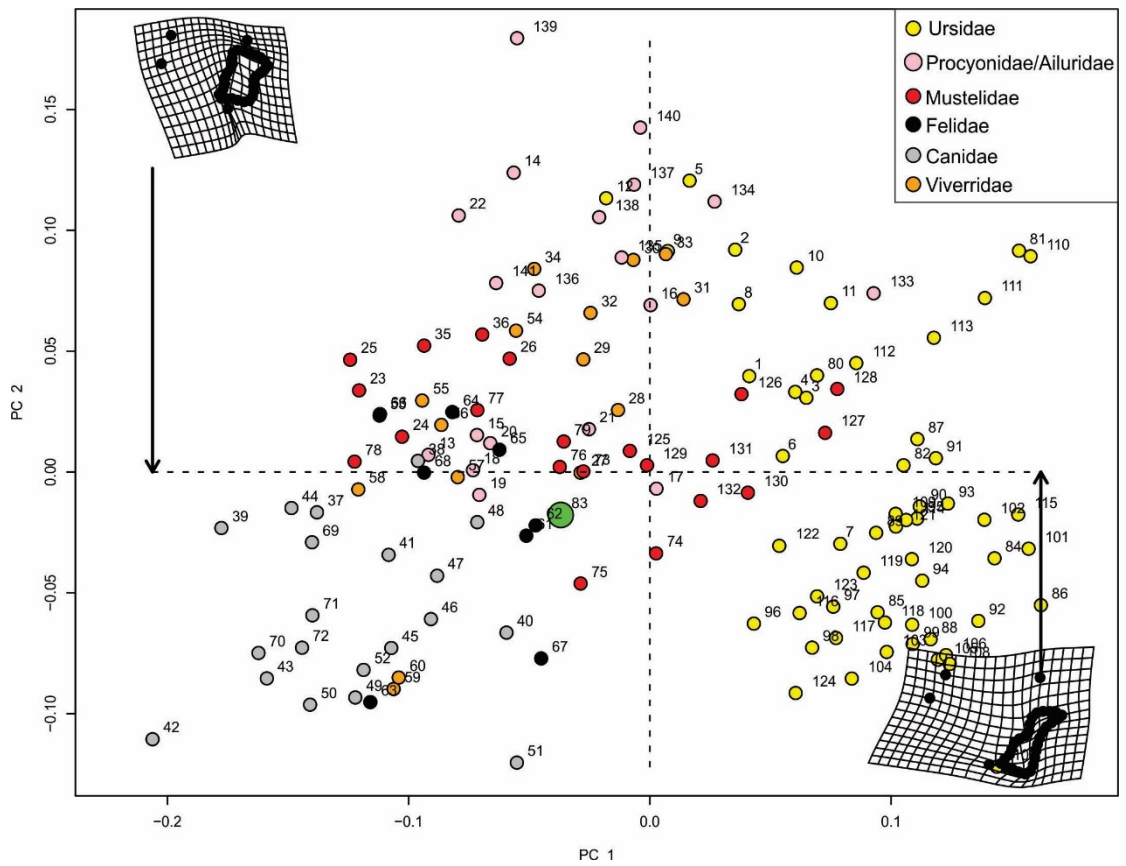


Fig. S15. Geometric morphometric analysis (PCA) of the distal humerus, categorized by families of Carnivora. Specimen numbers/taxa as in Fig. S12. Related to Fig. 4.

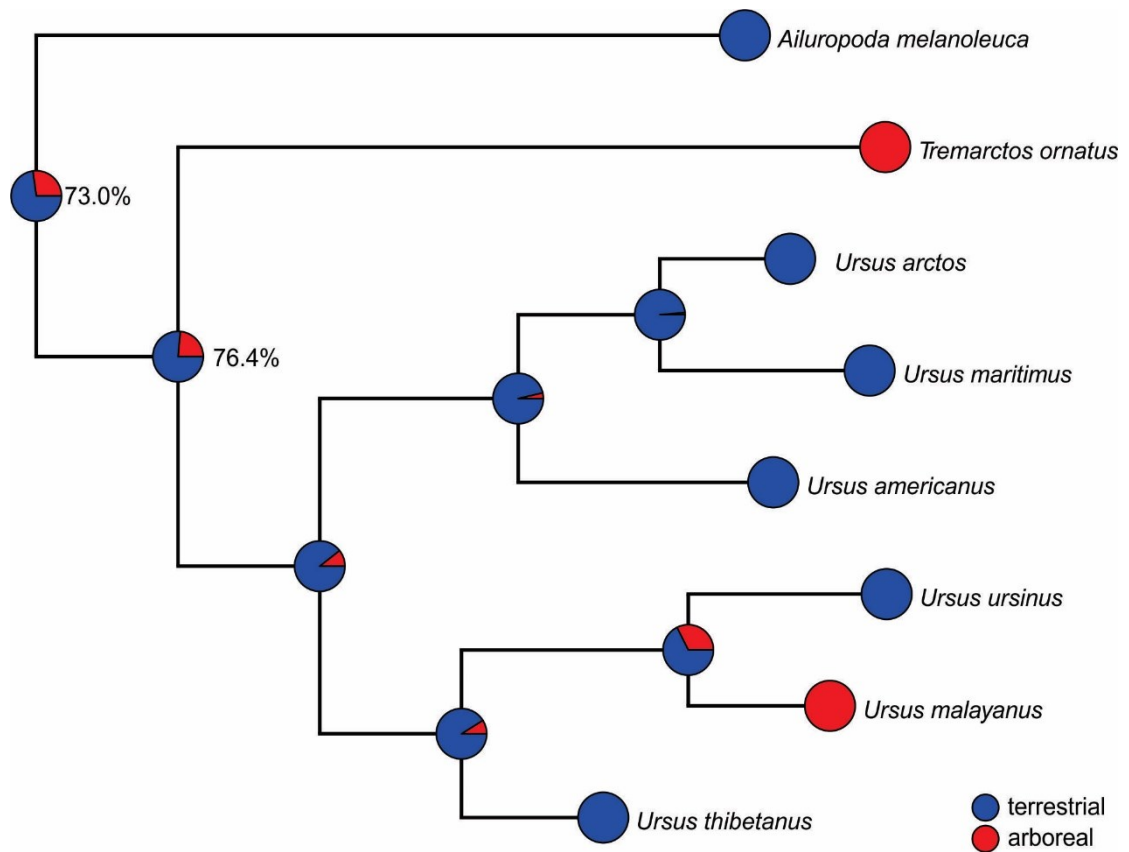


Fig. S16. Related to Fig. 4. Ancestor state reconstruction of lifestyle by maximum likelihood estimate using R package ape (Muda and Othman, 2015). *Tremarctos ornatus* and *Ursus malayanus* are viewed as arboreal in this analysis, even though they should be viewed as having a mixed habitat. From a parsimonious aspect, any species between the node of crown Ursidae and crown Ursinae would have a probability of terrestrial habit between 73.0%-76.4%.

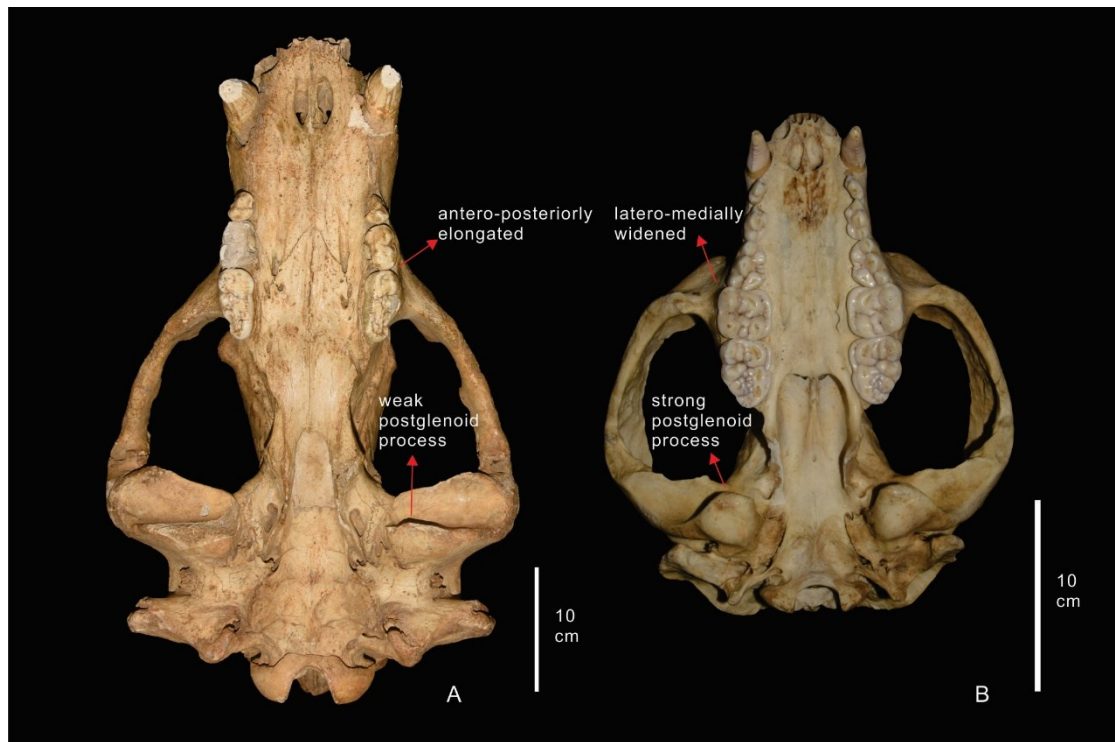


Fig. S17. Related to Fig. 5. Comparison of craniums of herbivorous bear. A. Cave bear *Ursus spelaeus*; B. giant panda *Ailuropoda melanoleuca*. Note the differences of dentition and postglenoid process.

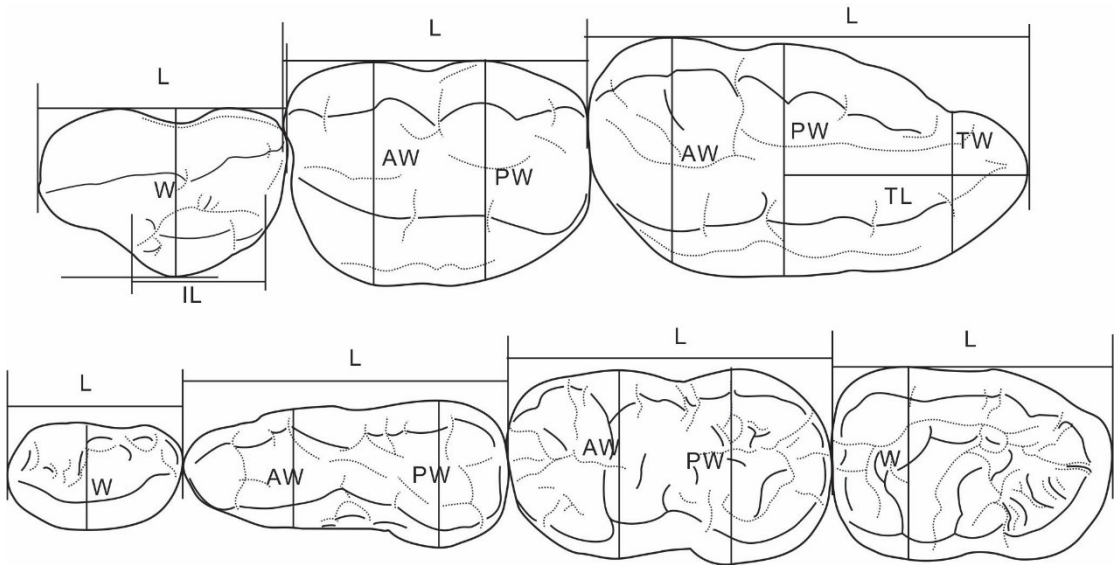


Fig. S18. Related to Fig. 5. Standards for dental measurements. Upper: P4, M1 and M2; Lower: p4, m1, m2 and m3.

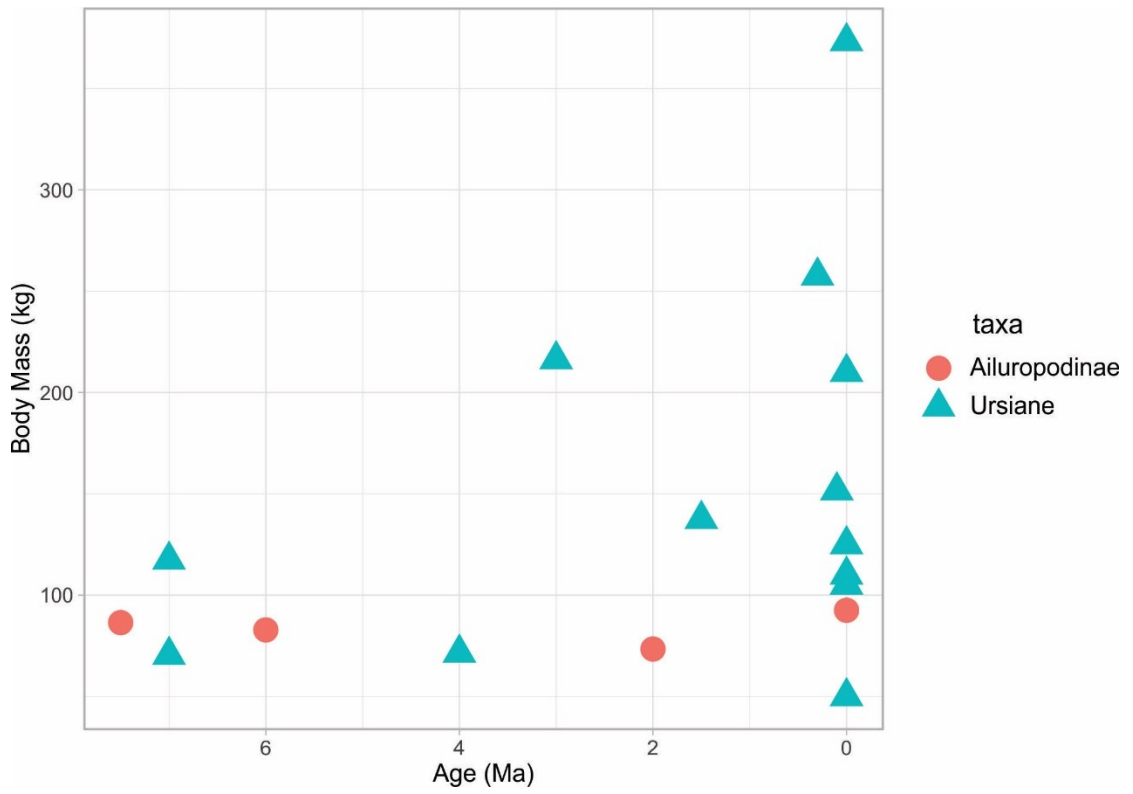


Fig. S19. Related to Fig. 5. Body mass evolution of plant-dominated omnivorous or herbivorous species of Ursinae and Ailuropodini.

Table S2. Related to Fig. 5. Ratios of dentition used for analyses. L. total length; mDm1. mandible depth behind the m1. Ridge represents the morphology of Rprd3, 0 represented the primitive state; 1 represents transitional state and 2 represents derived states (see Fig. 5 for details).

| Taxa | P4L/M1L | M2L/M1L | p4L/m1L | m2L/m1L | m3L/m1L | m1L/mDm1 | ridge |
|--------------------------------|---------|---------|---------|---------|---------|----------|-------|
| <i>Ballusia elmensis</i> | 1.05 | 0.95 | 0.60 | 0.71 | | 0.92 | 0 |
| <i>Ursavus brevirohinus</i> | 0.86 | 1.05 | | 0.73 | | | 0 |
| <i>Ursavus primaevus</i> | 1.06 | 1.34 | | 0.72 | 0.52 | | 0 |
| <i>Miomaci panonicum</i> | 0.89 | 1.00 | 0.44 | 0.74 | 0.46 | | 0 |
| <i>Indarctos atticus</i> | 1.07 | 1.18 | 0.50 | 0.76 | 0.49 | 0.74 | 0 |
| <i>Ailuropoda melanoleuca</i> | 1.06 | 1.39 | 0.67 | 0.79 | 0.55 | 0.80 | 0 |
| <i>Ursavus tirawa</i> | 0.96 | 1.02 | 0.46 | 0.79 | | 0.64 | 1 |
| <i>Ursavus tedfordi</i> | 0.82 | 1.14 | 0.50 | 0.81 | 0.55 | 0.56 | 1 |
| <i>Ursavus ehrenbergi</i> | 0.88 | 1.18 | 0.48 | 0.76 | 0.55 | | 1 |
| <i>Plionarctos harroldorum</i> | | | | 1.05 | 0.61 | | 1 |
| <i>Arctodus simus</i> | 0.87 | 1.44 | 0.37 | 0.94 | 0.65 | 0.50 | 1 |
| <i>Tremarctos floridanus</i> | 0.71 | 1.53 | 0.40 | 0.97 | 0.77 | 0.47 | 1 |
| <i>Tremarctos ornatus</i> | 0.75 | 1.40 | 0.45 | 0.99 | 0.71 | 0.58 | 1 |
| <i>Ursus thibetanus</i> | 0.69 | 1.53 | 0.52 | 1.02 | 0.77 | 0.53 | 2 |
| <i>Ursus malayanus</i> | 0.62 | 1.30 | 0.53 | 0.99 | 0.71 | 0.64 | 1 |
| <i>Ursus ursinus</i> | 0.73 | 1.14 | 0.62 | 0.91 | 0.63 | 0.39 | 1 |
| <i>Ursus americanus</i> | 0.66 | 1.49 | 0.52 | 1.06 | 0.83 | 0.56 | 2 |
| <i>Ursus etruscus</i> | 0.73 | 1.45 | 0.57 | 0.99 | 0.75 | 0.46 | 2 |
| <i>Ursus maritimus</i> | 0.83 | 1.40 | 0.62 | 0.98 | 0.76 | 0.45 | 2 |
| <i>Ursus arctos</i> | 0.72 | 1.61 | 0.54 | 1.04 | 0.86 | 0.52 | 2 |
| <i>Ursus spelaeus</i> | 0.71 | 1.63 | 0.52 | 1.15 | 0.97 | | 2 |
| <i>Ursus deningeri</i> | 0.70 | 1.76 | | 1.00 | 0.87 | | 2 |

Table S3. Related to Fig. 5. Body mass of selected Ursinae and Ailuropodinae.

| taxa | age | BM | group | source |
|---------------------------------|------|--------|---------------|-----------------------------------------------------------------|
| <i>Ursus thibetanus</i> | 0.00 | 125.00 | Ursinae | literature 53 |
| <i>Ursus malayanus</i> | 0.00 | 50.00 | Ursinae | literature 53 |
| <i>Ursus ursinus</i> | 0.00 | 105.00 | Ursinae | literature 53 |
| <i>Ursus americanus</i> | 0.00 | 110.00 | Ursinae | literature 53 |
| <i>Ursus arctos</i> | 0.00 | 210.00 | Ursinae | literature 53 |
| <i>Ursus spelaeus</i> | 0.00 | 373.28 | Ursinae | cubic to <i>U. arctos</i> |
| <i>Ursus deningeri</i> | 0.30 | 257.58 | Ursinae | cubic to <i>U. arctos</i> |
| <i>Ursus etruscus</i> | 1.50 | 137.50 | Ursinae | cubic to <i>U. arctos</i> |
| <i>Ursus minimus</i> | 3.00 | 216.32 | Ursinae | cubic to <i>U. thibetanus</i> |
| <i>Tremarctos ornatus</i> | 0.00 | 105.00 | Ursinae | literature 53 |
| <i>Tremarctos floridanus</i> | 0.10 | 151.61 | Ursinae | cubic to <i>T. ornatus</i> |
| <i>Ursavus tedfordi</i> | 7.00 | 70.43 | Ursinae | mean of cubic to <i>U. thibetanus</i> and <i>A. melanoleuca</i> |
| <i>Ursavus ehrenbergi</i> | 7.00 | 117.39 | Ursinae | mean of cubic to <i>U. thibetanus</i> and <i>A. melanoleuca</i> |
| <i>Plionarctos harroldorum</i> | 4.00 | 71.48 | Ursinae | mean of cubic to <i>U. thibetanus</i> and <i>A. melanoleuca</i> |
| <i>Ailurarctos yuanmouensis</i> | 7.50 | 86.43 | Ailuropodinae | mean of cubic to <i>U. thibetanus</i> and <i>A. melanoleuca</i> |
| <i>Ailurarctos lufengensis</i> | 6.00 | 82.82 | Ailuropodinae | mean of cubic to <i>U. thibetanus</i> and <i>A. melanoleuca</i> |
| <i>Ailuropoda microta</i> | 2.00 | 73.39 | Ailuropodinae | cubic to <i>A. melanoleuca</i> |
| <i>Ailuropoda melanoleuca</i> | 0.00 | 92.50 | Ailuropodinae | literature 53 |